UNIVERSITY OF CALIFORNIA, SAN DIEGO

Mechanisms of ARE-mediated gene repression by Tristetraprolin and homologs

A dissertation submitted in partial satisfaction of the requirements for the degree

Doctor of Philosophy

in

Biology

by

Rui Fu

Committee in Charge

Professor Jens Lykke-Andersen, Chair
Professor Amy Pasquinelli
Professor Jean Wang
Professor Miles Wilkinson
Professor Gene Yeo

2015

The Dissertation of Rui Fu is approved, and it is acceptable in quality and form for publication on microfilm and electronically:

_____

_____

_____

_____

_____

Chair

University of California, San Diego

2015

DEDICATION

This thesis is dedicated to my parents, 傅贤智, 杨青.

EPIGRAPH

“There is in all men a feeling of truth, which indeed is not sufficient in itself, but must be developed, proved, and purified; and to do this is the task of the Scholar.”

Johann Gottlieb Fichte, *The Vocation of the Scholar*

TABLE OF CONTENTS

LIST OF FIGURES AND TABLES

Chapter 2

Chapter 3

ACKNOWLEDGEMENTS

Chapter 2, in full, has been submitted for publication of the material as Fu R., Olsen M., Webb K., Bennett E., Lykke-Andersen J. The dissertation author was the primary investigator and author of this material.

Chapter 3, in part, is currently being prepared for submission for publication of the material as Fu R., Lykke-Andersen J. The dissertation author was the primary investigator and author of this material.

VITA

2009	Bachelor of Science, Xiamen University
2009–2015	Research Assistant, University of California, San Diego
2011–2013	Teaching Assistant, Division of Biological Sciences University of California, San Diego
2015	Doctor of Philosophy, University of California, San Diego

ABSTRACT OF THE DISSERTATION

Mechanisms of ARE-mediated gene repression by Tristetraprolin and homologs

by

Rui Fu

Doctor of Philosophy in Biology

University of California, San Diego, 2015

Professor Jens Lykke-Andersen, Chair

The zinc finger protein Tristetraprolin (TTP) promotes translation repression and degradation of mRNAs containing AU-rich elements (AREs). While much attention has been directed towards understanding the decay process and the machinery involved, the translation repression role of TTP has remained poorly understood. My thesis research identified the cap-binding translation repression 4EHP-GYF2 complex as a co-factor of TTP. Immunoprecipitation and *in vitro* pulldown assays demonstrate that TTP associates with the 4EHP-GYF2 complex via direct interaction with GYF2, and mutational analyses show that this interaction occurs via conserved tetraproline motifs of TTP. Mutant TTP with diminished 4EHP-GYF2 binding is impaired in its ability

to repress a luciferase reporter ARE-mRNA. 4ehp knockout mouse embryonic fibroblasts (MEFs) display increased induction and slower turnover of TTP target mRNAs as compared to wild-type MEFs. This work highlights the function of the conserved tetraproline motifs of TTP and identifies 4EHP-GYF2 as a co-factor in translational repression and mRNA decay by TTP.

The human genome encodes for two TTP homologs, BRF1 and BRF2, both of which are capable of ARE binding and decay activation. I observed that TTP family proteins are differentially regulated during serum-activated G_0-G_1-S transition in NIH 3T3 cells. The G_0-G_1-S cell cycle transition is regulated at multiple levels to avoid erroneous or mistimed cell proliferation. Transition over the G_0-G_1-S cell cycle requires repression of Retinoblastoma (RB) proteins, which are central components of the CDK-RB-E2F checkpoint pathway controlling in this transition. I identified ARE-containing *Rb*, *Rbl1* and *Rbl2* mRNAs encoding retinoblastoma proteins as targets of degradation by TTP family proteins. Depletion of TTP family proteins results in reduced expression of E2F transcription targets, and slower transition out of quiescence compared to control conditions. Together, this work demonstrates the involvement of mRNA decay in cell cycle progression.

Chapter 1. Introduction to TTP-mediated mRNA repression

1.1 Post-transcriptional processes regulate gene expression

Genetic information directs the synthesis of protein products through multiple steps (1). After transcription, the messenger (m)RNA transcript undergoes processing and transport into the cytoplasm, where ribosome assembly and active translation takes place. However, certain mRNA species can be stored in a reversible translationally repressed state, or marked irreversibly for mRNA turnover (2). While transcription and translation have been studied extensively, our understanding of mRNA decay regulation is more limited, but rapidly growing. In fact, recent global studies suggest mRNA decay rate regulations have significant contribution towards shaping rapidly induced and down-regulated mRNA level profiles (3, 4).

1.2 *Cis* elements and *trans* factors mediate regulated mRNA decay

mRNA decay can serve as a means of quality control by RNA surveillance systems. Alternatively, correctly transcribed and processed mRNAs also utilize decay pathways to fine-tune their expression levels in accordance with cellular conditions (5). In mammalian cells, controlled mRNA decay is usually initiated from deadenylation. This removal of the poly(A)-tail then either allows 3'-5' degradation by the exosome complex, or triggers decapping, followed by 5'-3' degradation by XRN1. Alternatively, mRNA can be cleaved by endonuclease activity, generating fragments that are then degraded by the exosome and XRN1 (6).

Regulatory potential is often encoded in the mRNA transcript as *cis*-elements, which are recognized by RNA-binding proteins that link decay machinery to the bound mRNA (7). These *trans* adaptors can be turned on or off through their own expression

and post-translational modifications, thus adapting mRNA decay to the needs of the cell.

For instance, AU-rich elements (ARE) in the 3'UTR of mRNAs are bound by numerous stabilizing or destabilizing proteins, whose availability vary depending on tissue type and cell signaling. Other mRNA *cis* elements, such as GU-rich elements recognized by CUGBP-1, micro-RNA target sites that interact with RNA-induced silencing complex (RISC), 3'UTR stem loop structures of histone mRNAs that interact with SLBP, and even long 3'UTRs recruiting UPF1, also promote mRNA instability (5).

1.3 ARE-binding proteins regulate expression of ARE-containing mRNAs

The AU-rich element is loosely defined, usually as repeats of the core pentamer AUUUA or nonamer UUAUUUAUU. It is predicted to reside in ~7% of all human genes, especially enriched for functional categories of cell communications, regulation of cell physiology, cell proliferation, nucleic acid metabolism, transcription and development, according to Gene Ontology analysis (8). The presence of 3'UTR AREs correlates with instability and repressed translation, two main processes of post-transcriptional regulation carried out by ARE-binding proteins (AUBPs).

AUBPs are a group of RNA-binding proteins that interact directly with the AREs. A case of convergent evolution, they encompass a wide variety of RNA-binding domains with specificity for similar sequences: CCCH zinc-finger domains for TTP, BRF1, and BRF2; KH domain for KSRP; RRM domains for AUF1, TIA-1, TIAR and HuR. On many mRNAs, AUBPs compete for the same AREs to exert different influences on transcript fate. HuR stabilizes bound mRNA, whereas TTP, BRF1, BRF2, AUF1, and KSRP induce rapid decay; HuR, TTP, and TIAR have also been reported to repress translation of their targets (8). Adding to the complexity, phosphorylation of

the stabilizing AUBP HuR leads to its translocation into the nucleus, and therefore inhibiting its binding to cytoplasmic mRNA (9); phosphorylation of TTP prevents its recruitment of deadenylation machinery; AUF1 is expressed in 4 isoforms, each with its unique RNA-binding affinity and effects on decay (10). Therefore depending on the specific tissue type or cell signaling state, cells can regulate the same ARE-containing transcript differently, as suited to their situation.

1.4 Tristetraprolin activates degradation of target mRNAs

The tandem zinc-finger protein Tristetraprolin was first discovered to be induced by TPA, insulin, and serum. Hence initially it was named TIS11 (TPA-inducible sequence 11), NUP475 (Growth factor-inducible nuclear protein 475), and G0S24 (G0/G1 switch gene 24). As its amino acid sequence revealed RNA-binding motifs and three striking tetraproline stretches, the protein was given more commonly used names ZFP36 (zinc finger protein 36) and TTP (Tris-tetra-prolin). Pioneering work from the Blackshear lab clarified a misconception that TTP was a transcription factor, as the zinc fingers were demonstrated to prefer single stranded RNA over DNA (11). However the tetraprolines, which were originally proposed to activate transcription, were never assigned any confirmed functions.

The tandem zinc fingers, each binding optimally to UUAU, are highly conserved from fish to mammals (12). Upstream of this RNA-binding domain is the N-terminal domain, which is known to interact with components of the Dcp2 decapping complex, the exonuclease Xrn1 and the exosome complex (13). The C-terminal domain contains a CNOT-interacting motif (CIM), which directly binds CNOT1, the large scaffold subunit of the CCR4-NOT deadenylase complex (14). Notably, the first tetraproline, but not the

second or third, is also highly conserved, again suggesting some conserved importance.

The function of TTP is highlighted by the knockout mouse phenotype. Homozygous TTP knockout mice appear normal upon birth, but soon develop autoimmunity and long-term inflammation. Most of the ailments can be alleviated by the injection of a TNFα antibody, pointing to a role in limiting TNFα expression for TTP (15). Evidence of TNFα as a TTP target is four-fold: TNFα mRNA levels are elevated in TTP knockout or knockdown cells; TNFα mRNA half-life is up-regulated in TTP KO or KD cells; TNFα mRNA co-purifies with TTP in immunoprecipitation experiments; TNFα mRNA contains conserved 3'UTR AREs. In the past decade, further efforts, especially ones aided by microarrays and RNA sequencing, have identified many more physiological targets of TTP (16-18).

Although the canonical view of TTP-mediated decay starts with deadenylation, followed by decapping and exonuclease degradation, TTP truncations without either the NTD or CTD, respectively deficient in decapping and deadenylation complex recruitment, still significantly destabilize bound mRNA (13). This suggests gene repression still occurs in the absence of either the decapping or deadenylation machinery. Alternatively, unknown factors may compensate for the loss of either interaction, or maybe the lost machinery undetectable by immunoprecipitation.is sufficiently recruited by weak indirect interactions.

1.5 TTP-mediated decay is regulated by expression and post-translational modifications

TTP target mRNAs are not necessarily always unstable. TTP protein itself is relatively unstable, with an approximate 30 min half-life (19). In the immune response,

where its regulatory activity is most studied, TTP is undetectable by western blot without stimulation. Upon immune response activation, both transcription and protein stability is temporarily up-regulated, orchestrating a burst of TTP protein, to target ARE-containing cytokines (20).

TTP can also be highly phosphorylated, with mass spectrometry data suggesting more than 10 sites on over-expressed TTP in cell culture (21). Of these candidate sites, S52, S178 and S323 (from human TTP) are phosphorylated by MK2 when the p38 pathway is active, and prevent deadenylase recruitment. The first two phosphoserines recruits 14-3-3 to TTP (22-24), whereas the third is located in the CIM (14), both presenting physical hindrance to CNOT1 binding. TTP is dephosphorylated by PP2A during the resolution phase of the innate immunity response (25), hence actively degrading target cytokine mRNAs to return the cell back to resting state. Dephosphorylation also destabilizes TTP protein, which reverts to undetectable levels when the immune response is shut down.

To date, phosphorylation of other sites have not been thoroughly studied, in terms of acting kinase and functional impact. Full length TTP and its C-terminal domain (CTD), but not the NTD, appear as hyperphosphorylated streaks on SDS-PAGE when exogenously expressed, yet both forms still possess gene repression activity. In addition, other modifications such as ubiquitination, may also modulate TTP activity (26).

1.6 Tristetraprolin mediates translational repression via poorly understood mechanisms

In addition to decay activation, TTP-tethering to reporter mRNAs leads to repressed translation, measured by reporter protein production and mRNA ribosome

profile (27). Depletion of TTP was reported to enhance translation of endogenous ARE-containing target mRNAs (28). Overall, we have very limited knowledge of TTP-mediated translation repression. The RNA-dependent helicase DDX6 (also called Rck/p54) was recently shown to participate in translational repression mediated by TTP (27), but no other co-factors or modulating signaling pathways have been discovered. Insight into translation repression mechanisms of other ARE-binding factors such as HuR and TIAR is also limited.

1.7 TTP homologs BRF1 and BRF2 also stimulate mRNA decay

The human genome encodes two homologs of TTP, named BRF1 (or ZFP36L1, Tis11b, ERF1) and BRF2 (or ZFP36L2, Tis11d, ERF2). Rodents express an additional TTP-homolog, ZFP36L3, whose expression is restricted to the placenta (29). The homologs and TTP share near identical zinc-finger motifs, and appear to bind the same core ARE. Similar to TTP, BRF1 and BRF2 also activate decay of bound transcripts, partly due to the conserved CIM (14), which recruits CNOT1 in TTP. In contrast to the immunity-related phenotypes of TTP knockout mice, knockout of BRF1 is embryonic lethal (30), and BRF2 knockout mice die shortly after birth (31). Consistent with important developmental roles, BRF1 and BRF2 were both recently implicated in the regulation of pluripotency and differentiation, through destabilizing target transcripts (32, 33).

The homologs exhibit partial overlapping yet distinct expression patterns in tissues. TTP is most highly expressed in the liver, kidney, testis and ovary (34); for BRF1, liver, pancreas, ovary, testis, prostate and placenta; for BRF2, B and T cells, pancreas and ovary (35). Target specificity also appears to be partially overlapping between the homologs, but overexpression of one homolog does not fully compensate

for the deficiency of another. For example, deletion of both BRF1 and 2, but not either single deletion, in T cells results in acute leukemia in mice, as both proteins regulate Notch1 expression (36). On the other hand, even though TTP and BRF1 proteins are expressed at higher levels than BRF2 in the ovary, BRF2 mutation leads to anovulation not rescued by normal or over-expression of the other homologs (37). Furthermore, how the TTP homologs coordinate to regulate shared targets is unclear.

Overall, decades more of research has been conducted on TTP than on its homologs. Therefore our knowledge on TTP offers some directions into investigations of BRF1 and BRF2. Similar to p38-MK2 regulation of TTP, BRF1 phosphorylation by PKB on residues S92 and S203 also promotes binding of 14-3-3, blocks deadenylase recruitment, and stabilizes the protein (38). Although BRF2 protein is also inherently unstable (39), post-translational modification pathways regulating BRF2 activity and stability have not been identified. In addition, whether BRF1 and BRF2 repress translation similar to TTP is unclear.

Curiously, birds do not appear to encode an ortholog of TTP, nor TNFα. While BRF and BRF2 are present in birds, they do not appear to mirror the expression pattern nor function of TTP in other organisms. Interestingly, the primary TTP target TNFα, as is also not found in birds. In contrast, orthologs of several other TTP-targeted cytokines such as GM-CSF and IL10 do exist in chicken, and they each contain at least one potential AU-rich element. How birds have evolved into a different strategy of coping with pathological insults remains a fascinating question (40).

Chapter 2. Tristetraprolin recruits the 4EHP-GYF2 cap-binding complex to repress and degrade mRNAs with AU-rich elements

2.1 Introduction

The translation and degradation of mRNAs are central, interrelated steps in the control of gene expression. Both processes are impacted by general mRNA-associated factors. The cap-binding translation initiation complex eIF4F serves to promote translation initiation, while preventing access to the mRNA cap for the Dcp2 decapping complex (41). Cytoplasmic Poly(A)-binding protein (PABPC) stimulates translation initiation while impacting mRNA deadenylation through repression or stimulation of deadenylase complexes (42). Consistent with this relation between translation initiation and mRNA stability, many RNA binding proteins (RBPs) that promote mRNA degradation also repress translation initiation (43-45). However, the underlying mechanisms remain poorly understood.

A subset of translation repressors inhibits translation at the initiation step by interfering with the eIF4F complex. This includes, eIF4E binding proteins (4EBPs) that bind to eIF4E in competition with eIF4G thereby repressing translation initiation by inhibition of eIF4F complex formation (46, 47). 4E-T is another eIF4E binding protein, which inhibits translation initiation by a less well-defined mechanism (48). Furthermore, a class of *S. cerevisiae* RGG-domain proteins associate with eIF4G to represses translation (49). Another factor that interferes with cap-dependent translation is 4EHP (also known as eIF4E2). 4EHP is a homolog of eIF4E and is thought to repress translation by competition with the eIF4F complex for binding to the mRNA cap (50, 51). Drosophila 4EHP was identified as a co-factor of the RNA-binding protein Bicoid required for translation repression of *caudal* mRNA (52). Mammalian 4EHP has been reported to form translation repression complexes with GYF1/GYF2 (also known as

GRB10 interacting GYF protein 1/2) co-factors (53), but mRNA-specific recruitment of 4EHP-GYF complexes by RBPs has not been previously identified in mammals.

Tristetraprolin (TTP; also known as ZFP36 or Tis11) is an RBP that represses translation and activates degradation of mRNAs containing 3'UTR AU-rich elements (AREs) (11). TTP plays an important role in attenuating cytokine expression during immune responses via repression and degradation of ARE-containing cytokine mRNAs (17, 54, 55). In the mouse, TTP knockout results in auto- and hyper-immunity due to over-production of the cytokine TNFα, which is produced from an ARE-containing mRNA (15). TTP binds AREs through its tandem Zn-finger RNA binding domain, and recruits the Dcp2 decapping complex (13, 56), the CCR4-NOT deadenylase complex (13, 14, 57, 58) as well as exonucleases (13, 59, 60). The activity of TTP is controlled through phosphorylation by the p38-MK2 pathway, which inhibits recruitment of the CCR4-NOT deadenylase complex and prevents cytokine mRNA degradation during early stages of an immune response (22-24, 61). In addition to activation of mRNA decay, TTP also promotes translation repression, which appears to be the dominant mechanism of repression by TTP under certain conditions (28). The helicase DDX6 (also called Rck/p54) was recently implicated in translation repression by TTP (27), but the specific mechanism of TTP-mediated translation repression has remained poorly understood.

The RNA binding zinc finger domain and a C-terminal CCR4-NOT interaction motif (CIM) are highly conserved regions of TTP. Another evolutionary conserved feature of TTP is its tetraproline (PPPPG) motifs, which served as the basis for the naming of the protein (62). However, the functional significance of these motifs has remained unknown. Two paralogs of TTP exist in the human genome, BRF1 (also known as ZFP36L1 and Tis11b) and BRF2 (ZFP36L2, Tis11d), which, like TTP,

promote degradation of ARE-containing mRNAs (32, 63, 64). These proteins share the conserved zinc finger and CIM domains with TTP, but lack the tetraproline motifs characteristic of TTP.

In this study, we identify the translation repression complex 4EHP-GYF2 as a TTP co-factor. Our interaction studies *in vitro* and in cells demonstrate that TTP associates with the 4EHP-GYF2 complex via direct interaction with the GYF2 subunit. Mutational studies reveal that the interaction occurs through conserved tetraproline motifs of TTP. Mutation of TTP tetraproline motifs and knockout of 4EHP in mouse embryonic fibroblasts resulted in deficiencies in TTP-mediated mRNA repression at both the translational and mRNA turnover level. These findings are consistent with a role of 4EHP in TTP-mediated translation repression as was very recently reported (65). Moreover, our study identifies GYF2 as the factor that bridges 4EHP to TTP via interaction with the characteristic TTP tetraproline motifs, and suggests that the 4EHP-GYF2 complex links translation repression by TTP with mRNA decay.

2.2 Results

The 4EHP-GYF2 translation repression complex associates with TTP

To identify candidate TTP co-factors we performed immunoprecipitation (IP) against endogenous TTP at different time points during a lipopolysaccharide (LPS)-stimulated innate immune response in mouse RAW264.7 macrophages and subjected samples to liquid chromatography followed by tandem mass spectrometry (LC/MS-MS). IPs were performed in the presence of RNase A to prevent co-purification of proteins that associate with TTP in an RNA-dependent manner. Anti-TTP IP prior to LPS induction where TTP levels are low (t=0), and IP using normal rabbit serum (NRS) served as negative controls (Figure 2.1A). As expected, we observed all components

of the CCR4-NOT deadenylase complex in association with TTP, with the exception of NOT4 which is often absent from CCR4-NOT complexes (66) (Figure 2.2). In addition, multiple 14-3-3 proteins and hnRNP F were also detected in association with TTP consistent with previous observations (22, 67, 68) as were subunits of phosphatase 2A (PP2A), consistent with previous reports of TTP dephosphorylation by PP2A (25). Intriguingly, in addition to previously identified TTP-associated factors, our LC/MS-MS analysis identified the eIF4E homolog 4EHP and the 4EHP-associated GYF-domain protein GYF2 in association with TTP (Figure 2.1A). The GYF2-paralog GYF1 was also found associated with TTP but only at modest levels. These associations were all specific to TTP as they were minimal in both of the negative control IPs (Figure 2.1A, and 2.2). Not all factors known to complex with TTP were captured by this approach; for example decapping and exosome components, previously observed in complex with TTP by co-IP (13, 59, 60) , were not detected above background in our IP LC/MS-MS data.

TTP interacts with the 4EHP-GYF2 complex via a direct interaction with GYF2

To test whether the 4EHP-GYF2 complex serves as a co-factor for TTP in mRNA repression, we first sought to further characterize the association between TTP and the 4EHP-GYF2 complex. Of the two GYF proteins we focused entirely on GYF2 given the low level of peptide recovery for GYF1 in our IP-LC/MS-MS assays. Consistent with our IP-LC/MS-MS data, myc-tagged mouse TTP could be observed to co-purify in an RNA-independent manner with FLAG-tagged mouse 4EHP and GYF2 when transiently co-expressed in human embryonic kidney (HEK) 293T cells (Figure 2.1B).

To test whether the interaction between TTP and 4EHP-GYF2 is direct, we produced Glutathione-S-Transferase (GST)-tagged mouse TTP and His_6-tagged mouse 4EHP and GYF2 recombinantly in *Escherichia coli* for use in *in vitro* pull down assays. This uncovered an interaction between TTP and GYF2 that was independent of 4EHP (Figure 2.1C). A weak interaction could also be observed between TTP and 4EHP in some experiments, but this interaction was strongly enhanced by GYF2 (Figure 2.1C and 2.4). Therefore, complex formation between TTP and 4EHP-GYF2 is mediated primarily by a direct interaction between TTP and GYF2 with a possible minor contribution from an additional TTP-4EHP interaction (Figure 2.1D).

GYF2 interacts with TTP via TTP tetraproline motifs

Next, to map the domain(s) of TTP important for interaction with 4EHP-GYF2, we transiently expressed domain truncation mutants of mouse TTP in HEK293T cells and monitored for effects on association with 4EHP and GYF2 by co-IP. The N-terminal domain (NTD) of TTP was necessary and sufficient for 4EHP and GYF2 association, as deletion of the TTP NTD (ΔNTD) resulted in loss of 4EHP and GYF2 association, whereas the TTP NTD alone retained 4EHP-GYF2 association (Figure 2.5). The CIM sequence of TTP, responsible for interaction with the CCR4-NOT complex (14), did not contribute to 4EHP-GYF2 binding. Further deletion analyses revealed that the last 33 amino acids of the TTP NTD (TTP_{61-93}) are sufficient for association with 4EHP and GYF2 (Figure 2.6).

GYF domains are known as protein interaction domains with specificity for the amino acid sequence PPPGφ, with φ representing a hydrophobic residue (69, 70). Mammalian TTP contains three tetraproline motifs, two of which are followed by GF or GL, matching the PPPGφ consensus (Figure 2.7A). Sequence alignment of

mammalian TTP with other vertebrates revealed strong conservation of a PPPGφ motif overlapping with the first tetraproline motif, which is located near the C-terminal end of the TTP NTD (aa 63-68), within the minimal region of TTP associating with 4EHP-GYF2 (Figure 2.7A). Tetraproline motif 2 residing in the TTP CTD is less conserved but also matches a PPPGφ consensus in many vertebrates including human and mouse, whereas tetraproline motif 3 is poorly conserved and fails to match a PPPGφ consensus (Figure 2.7A). Mutation of the conserved prolines of tetraproline motif 1 to serines dramatically decreased 4EHP and GYF2 association with full-length mouse TTP as well as with TTP NTD and TTP_{61-93} (Figure 2.7B). Mutation of the GF sequence that follows the tetraprolines to DE reduced association of the TTP NTD and TTP_{61-93} with 4EHP-GYF2, but had little effect in the context of full-length TTP, suggesting that this mutation is less disruptive to the interaction.

Combining P to S mutations in tetraproline motifs 1, 2 and 3 revealed that motif 2 contributes to 4EHP-GYF2 association, as mouse TTP containing mutations in both of motifs 1 and 2 showed decreased association with 4EHP-GYF2 as compared with TTP mutated in motif 1 alone (Figure 2.8A). By contrast, we observed no contribution from motif 3, consistent with the absence of a hydrophobic residue following the PPPG sequence in this motif (Figure 2.7A). The importance of TTP tetraproline motifs 1 and 2 for the interaction with GYF2 was confirmed *in vitro*, as P to S mutations in these motifs resulted in loss of GYF2 interaction (Figure 2.8B). Consistent with the tetraproline motifs of TTP serving as the primary site of interaction with the 4EHP-GYF2 complex, we observed little association of GYF2 with TTP paralogs BRF1 and BRF2, which lack PPPGφ motifs (Figure 2.8C).

Tetraproline motifs 1 and 2 and 4EHP contribute to TTP-mediated mRNA repression

To test whether TTP tetraproline motifs 1 and 2 contribute to TTP activity we took advantage of TTP knockout mouse embryonic fibroblasts ($TTP^{-/-}$ MEFs; (16)) to test the ability of mutant TTP proteins to repress an ARE-containing luciferase reporter mRNA. Wild-type or mutant TTP were transiently co-expressed in the $TTP^{-/-}$ MEFs with a firefly luciferase reporter containing the ARE of human GM-CSF mRNA. *Renilla* luciferase lacking an ARE served as a normalization control. As expected, wild-type TTP greatly repressed firefly luciferase expression (Figure 2.9A). Mutations in tetraproline motifs 1 and 2 reduced the ability of TTP to repress the luciferase ARE-reporter mRNA despite this protein being expressed at similar levels as WT TTP (Figure 2.9B). As expected, deletion of the CIM domain also reduced TTP activity. mRNA level measurements using qRT-PCR revealed similar levels of luciferase mRNA in each sample (Figure 2.10) arguing that the primary effect of TTP on the luciferase reporter in these assays is at the level of translation repression. The absence of a complete loss of TTP function associated with mutations in the tetraproline and CIM motifs is consistent with the ability of TTP to recruit multiple repression complexes via different domains (13, 14).

To more directly test the importance of 4EHP in ARE-mRNA repression, we turned to $4EHP^{-/-}$ MEFs (53). Consistent with 4EHP-GYF2 playing a role in ARE-mRNA repression, increased luciferase activity is observed from the firefly luciferase ARE-reporter in $4EHP^{-/-}$ MEFs as compared to MEFs from $4EHP^{+/+}$ littermates (Figure 2.9C). Importantly, reintroduction of exogenous 4EHP and GYF2 into the knockout cell line partially rescued this increase in expression; GYF2 was co-expressed with 4EHP in this rescue experiment since GYF2 levels were previously reported to be low in the

4EHP$^{-/-}$ MEFs. These findings are consistent with a recent report of 4EHP playing a role in TTP-mediated translation repression (65).

Endogenous TTP-target mRNAs are stabilized in 4EHP knockout MEFs

We next tested the importance of 4EHP for repression of endogenous TTP-target mRNAs using the 4EHP$^{-/-}$ MEFs (53). Serum addition is a well-described stimulation that induces TTP and TTP-target mRNAs in MEFs (16, 62). We therefore monitored the induction of known TTP-target mRNAs during a time course of six hours of serum stimulation following serum starvation in 4EHP$^{-/-}$ MEFs as compared to the MEFs from 4EHP$^{+/+}$ littermates (16). This revealed strongly enhanced induction in 4EHP$^{-/-}$ MEFs of *Ier3*, *Csf2*, and *Cxcl10* mRNAs, all ARE-containing mRNAs known to be regulated by TTP (Figure 2.11A). By contrast, *Fos* mRNA, which is regulated in a TTP-independent manner (16, 71), was unaffected by 4EHP knockout. The increased induction of TTP-target mRNAs in 4EHP$^{-/-}$ MEFs occurred despite TTP mRNA and protein induction being similar, and possibly slightly higher, in the 4EHP$^{-/-}$ as compared to the 4EHP$^{+/+}$ MEFs (Figure 2.11B).

The observation of increased accumulation of TTP-target mRNAs in 4EHP$^{-/-}$ MEFs suggested a possible effect of 4EHP on mRNA decay. Indeed, Actinomycin D-mediated transcription shutoff mRNA decay assays performed 2 hours after serum induction revealed that *Ier3*, *Csf2* and *Cxcl10* mRNAs are all stabilized in 4EHP$^{-/-}$ as compared to the 4EHP$^{+/+}$ littermate MEFs (Figure 2.12). By contrast, *Fos* and histone *Hist2h2aa1* mRNAs, which undergo rapid decay independently of TTP, did not show reduced decay rates in 4EHP knockout MEFs. Collectively, our observations suggest that the 4EHP-GYF2 complex is an important co-factor in the repression of ARE-

mRNAs by TTP and that 4EHP-GYF2 contributes to both translation repression and mRNA decay.

2.3 Discussion

In this study, we have identified the 4EHP-GYF2 translation repression complex as a co-factor of TTP (Figure 2.13). TTP associates with the 4EHP-GYF2 complex via direct interaction with GYF2 as evidenced by *in vitro* pull-down assays using *E. coli* produced proteins (Figure 2.1C and 2.8B). The conserved first and second tetraproline motifs of TTP are necessary for maintaining direct interaction with GYF2, both in transfected mammalian cells and in *in vitro* pull-down assays (Figure 2.8). The 4EHP-GYF2 complex contributes to TTP-mediated mRNA repression as evidenced by mutations in TTP tetraproline motifs and deletion of 4EHP derepressing an ARE-containing luciferase reporter mRNA and by the accumulation and stabilization of TTP-target mRNAs induced during serum activation of $4EHP^{-/-}$ MEFs (Figure 2.10, 2.11 and 2.12). Given the evolutionary conservation of TTP tetraproline motifs (Figure 2.6A), the role of the 4EHP-GYF2 complex in TTP function is likely conserved in vertebrates. Interestingly, unlike the association with the CCR4-NOT deadenylase (23, 24), we found no effect of the phosphatase 2A (PP2A) inhibitor okadaic acid on the association of TTP with 4EHP-GYF2 (Figure 2.14), suggesting that TTP-4EHP-GYF2 complex formation is not regulated by phosphorylation.

How does the 4EHP-GYF2 complex contribute to TTP activity? In addition to activating mRNA degradation, TTP has been demonstrated to promote translation repression, which might be the predominant mechanism of TTP-mediated repression in some conditions (27, 28). 4EHP was recently reported to stimulate translation repression mediated by TTP (65), which is consistent with the reported function of

Drosophila 4EHP and the mammalian 4EHP-GYF2 complex in translation repression (52, 53). Consistent with this, we found that mutation in tetraproline motifs 1 and 2 reduced the ability of TTP to associate with 4EHP-GYF2 (Figure 2.8) and to repress a luciferase ARE-reporter (Figure 2.9). 4EHP knockout also resulted in derepression of the luciferase ARE-reporter (Figure 2.9C), but in addition, triggered accumulation and stabilization of TTP-target mRNA in serum-activated MEFs (Figure 2.11 and 2.12). Therefore, in addition to stimulating translation repression, 4EHP-GYF2 also contributes to TTP-mediated mRNA degradation. One possibility is that 4EHP-GYF2 directly links repression of translation initiation with mRNA degradation by interfering with the eIF4F complex to promote a remodeling step that helps expose the mRNA cap to decapping. Alternatively, the increased accumulation and stabilization of TTP-target mRNAs in serum-stimulated 4EHP knockout MEFs could be a secondary effect of a failure in TTP-mediated translation repression, for example if increased translation of TTP-target mRNAs results in delayed attenuation of the serum activation response.

Our findings add a new layer of complexity to TTP-mediated mRNA regulation. In previous studies, TTP has been found to associate with and activate the exosome (60) and the Dcp2 decapping (13) and CCR4-NOT deadenylase complexes (13, 14). Consistent with the ability to activate multiple mRNA repression and degradation factors, multiple domains and motifs of TTP have been found to contribute to TTP function (13, 72) including the tetraproline motifs as identified in this study (Figure 2.13). This ability to engage multiple mRNA repression and degradation machineries appears to be an emerging general principle in mRNA regulation by RBPs. For example Upf1, the central component of the nonsense-mediated decay pathway, is known to associate with multiple degradation factors (73-75). The microRNA-guided RISC complex can also both activate degradation and repress translation (76). Similarly, PUF

proteins are known to repress and degrade mRNAs by recruitment of multiple co-factors (77, 78). Thus, the ability to recruit multiple repression factors might be an important general feature of RBPs that promote mRNA repression. This could serve as a mechanism to efficiently activate sequential steps in mRNA repression and degradation. Alternatively, co-factors could be individually sufficient for mRNA repression, allowing the RBPs to carry out mRNA repression and/or degradation in different tissues using different available co-factors.

2.4 Figures

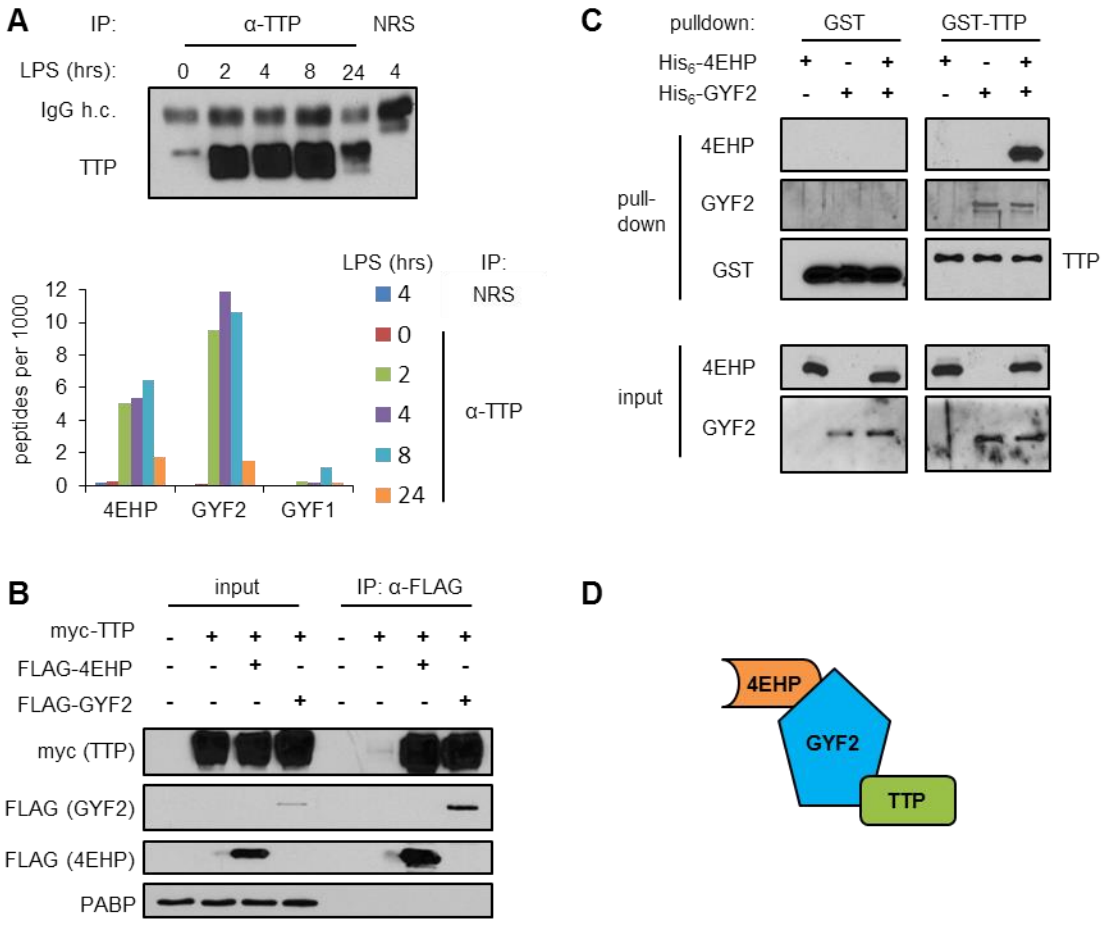

Figure 2.1. TTP interacts with the 4EHP-GYF2 complex. (A) Top: Western blot for TTP in samples immunoprecipitated with anti-TTP or normal rabbit serum (NRS) from mouse macrophage RAW264.7 cells treated with lipopolysaccharide (LPS) for various lengths of time as indicated. IgG h.c.: IgG heavy chain. Bottom: graph showing the number of peptides for 4EHP, GYF2 and GYF1 detected per 1000 of total detected peptides in LC/MS-MS analyses of the IPs. **(B)** Western blots of input and anti-FLAG IPs from HEK293T cells co-transfected with myc-TTP and FLAG-4EHP or FLAG-GYF2. Lysates were treated with RNase A prior to IP. **(C)** Western blots monitoring His_6-4EHP and His_6-GYF2 interaction with GST or GST-TTP in *in vitro* pull-down assays using glutathione Sepharose beads. GST and GST-TTP were detected using anti-GST; 4EHP and GYF2 were detected using anti-4EHP and anti-GYF2, respectively. **(D)** Proposed model of interaction between TTP and the 4EHP-GYF2 complex. TTP directly binds GYF2, which is known to interact with 4EHP.

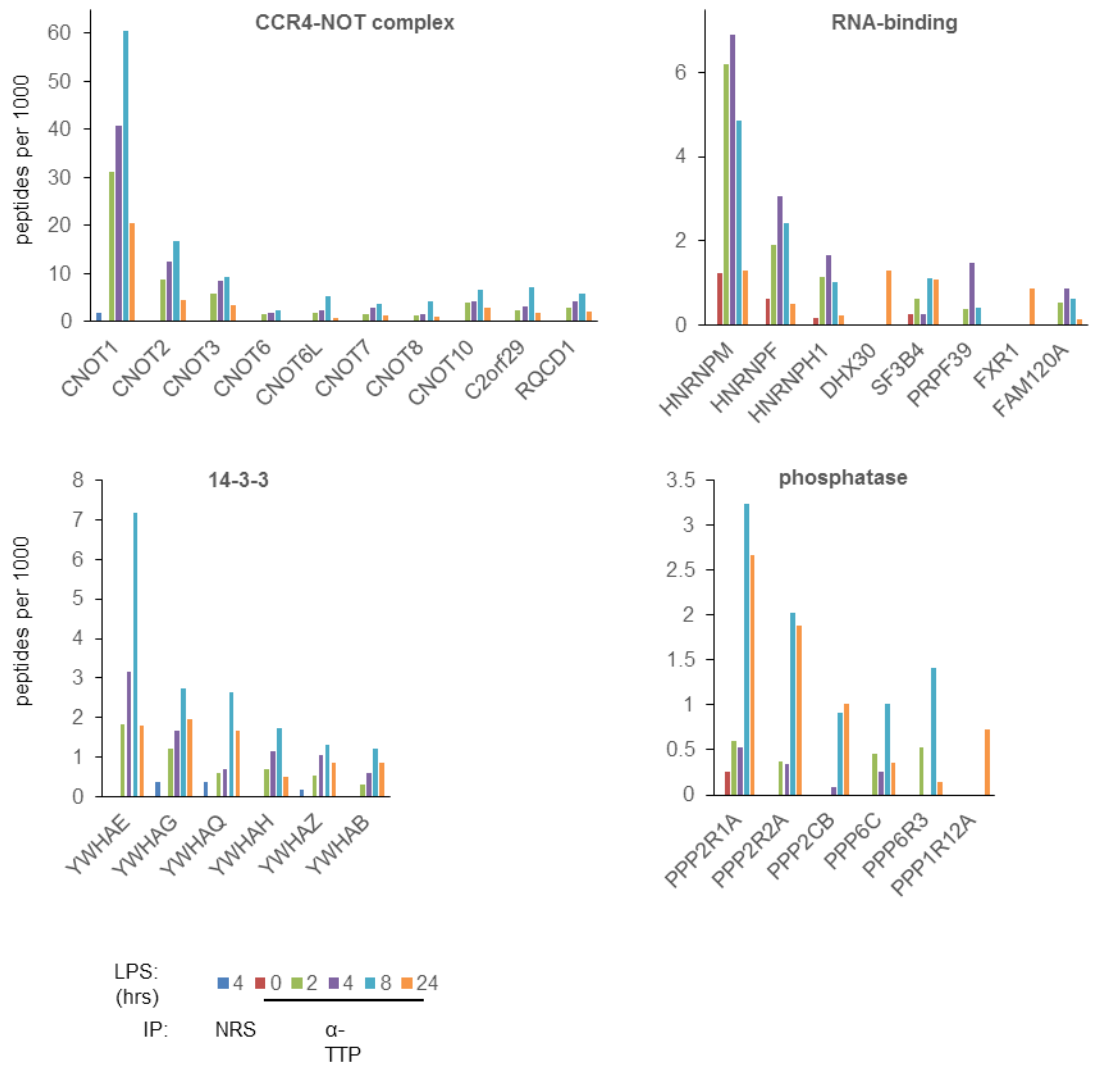

Figure 2.2. Proteins enriched in the TTP IP LC/MS-MS analysis sorted by groups. Graphs showing the fraction of peptides (per 1000) for all proteins whose maximum number of peptides counted in the 2, 4, 8, 24 hr anti-TTP samples is at least 10, and at least 4-fold enriched in the fraction of peptides in the sample over the fraction in each of the negative control samples (NRS and 0 hr LPS anti-TTP samples). Bars in the graphs are color coded according to the time-points they represent as indicated in the legend.

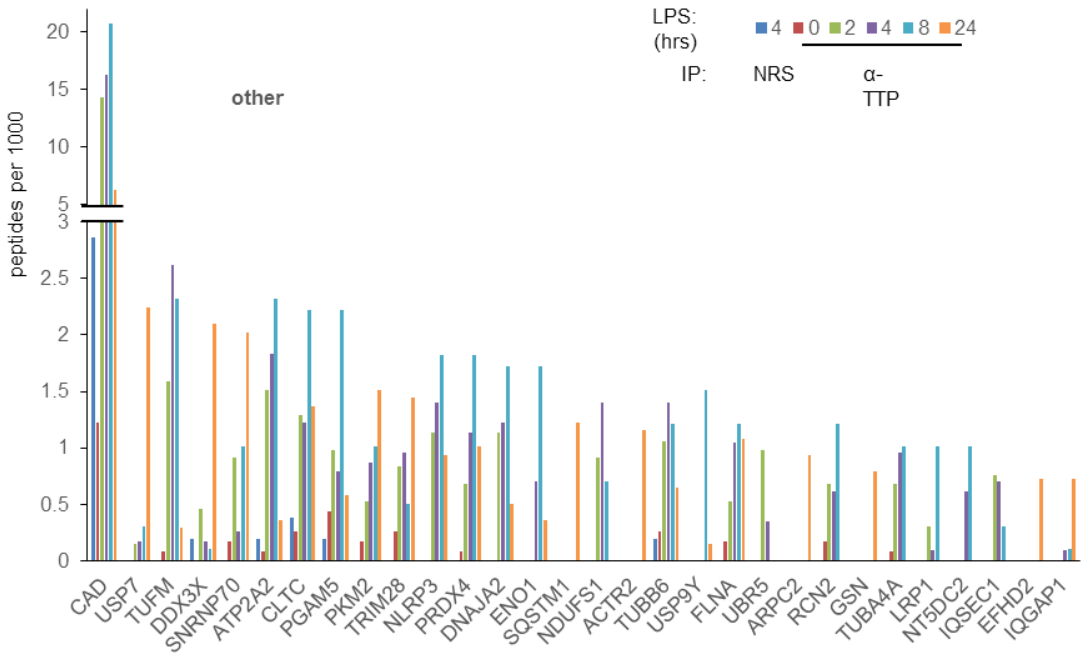

Figure 2.3. Various other proteins enriched in the TTP IP LC/MS-MS analysis. Graphs showing the fraction of peptides (per 1000) for all proteins whose maximum number of peptides counted in the 2, 4, 8, 24 hr anti-TTP samples is at least 10, and at least 4-fold enriched in the fraction of peptides in the sample over the fraction in each of the negative control samples (NRS and 0 hr LPS anti-TTP samples). Bars in the graphs are color coded according to the time-points they represent as indicated in the legend.

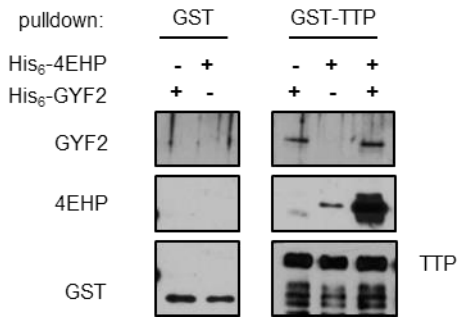

Figure 2.4. The interaction between 4EHP and TTP is greatly enhanced by GYF2. *In vitro* pulldown of His_6-4EHP and/or His_6-GYF2 after GST or GST-TTP were incubated with glutathione beads similar to the experiment in Figure 2.1C.

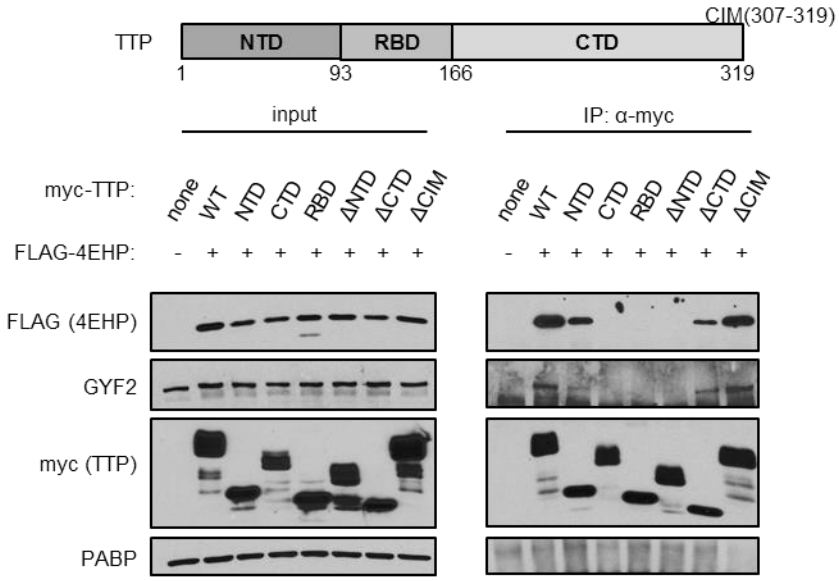

Figure 2.5. The TTP N-terminal domain is necessary and sufficient for association with 4EHP and GYF2. Western blots for indicated factors in input and anti-myc IP fractions from RNase A-treated extracts of HEK293T cells transiently expressing indicated myc-tagged TTP variants and FLAG-tagged 4EHP. A schematic of TTP is shown at the top indicating the N-terminal domain (NTD), the RNA-binding domain (RBD), the C-terminal domain (CTD) and the CNOT-Interacting Motif (CIM).

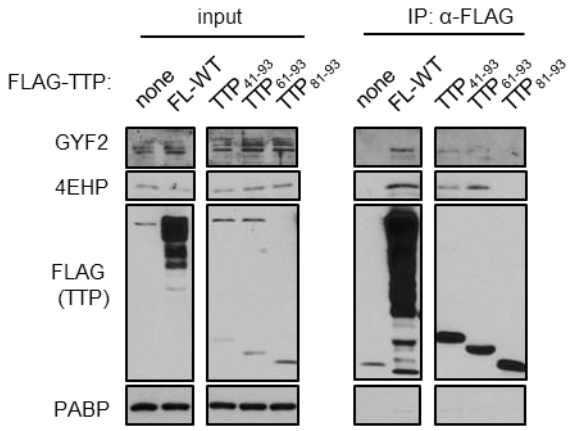

Figure 2.6. Amino acids 61-93 of TTP are sufficient for association with 4EHP and GYF2. Western blots of input and anti-FLAG IP samples from RNase A-treated extracts of HEK293T cells transiently expressing indicated mouse TTP variants. FL-WT: Full-length wild-type TTP. TTP_{41-93}, TTP_{61-93}, TTP_{81-93}: fragments of TTP fused at their N-terminus with a FLAG-tag and MS2 coat protein.

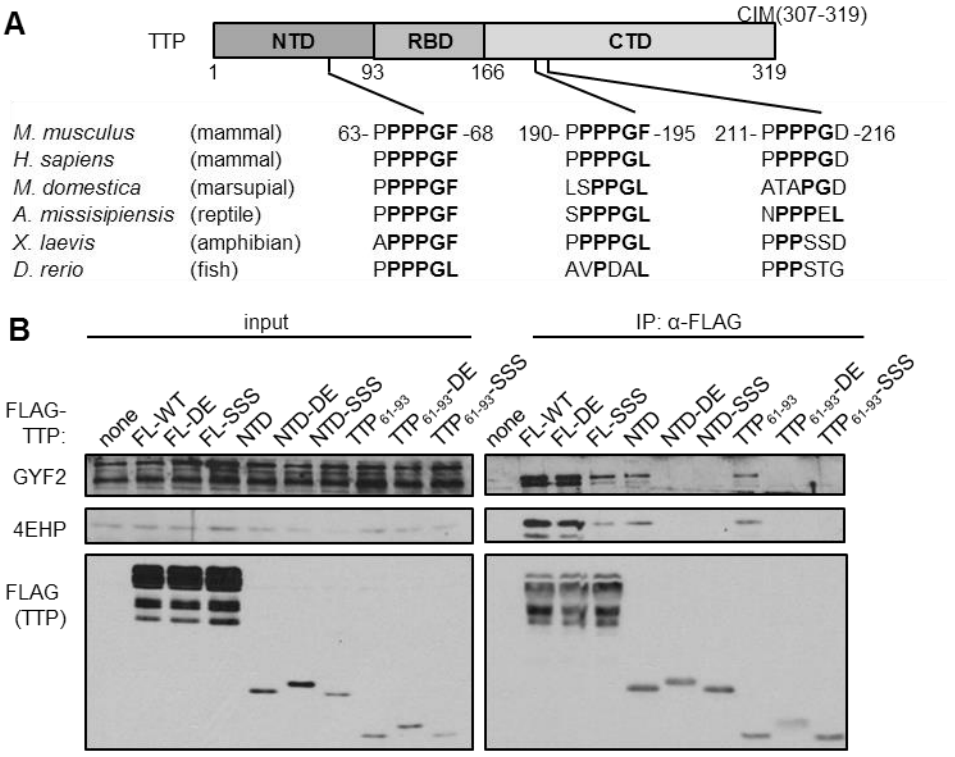

Figure 2.7. TTP interacts with GYF2 through the NTD tetraproline motif. (A) Sequence alignment of the tetraproline motifs of mouse TTP with corresponding regions of TTP from other vertebrates. Amino acids matching the PPPGφ GYF-binding consensus are highlighted in bold. **(B)** Western blots for proteins indicated on the left in input and anti-FLAG IP samples from RNase A-treated extracts of HEK293T cells transiently expressing indicated FLAG-tagged TTP variants. The first PPPPGF motif of TTP was mutated to PSSSGF (SSS) or PPPPDE (DE) in the contexts of full length TTP (FL), the TTP NTD, or the 33 amino acids surrounding the motif (TTP_{61-93}).

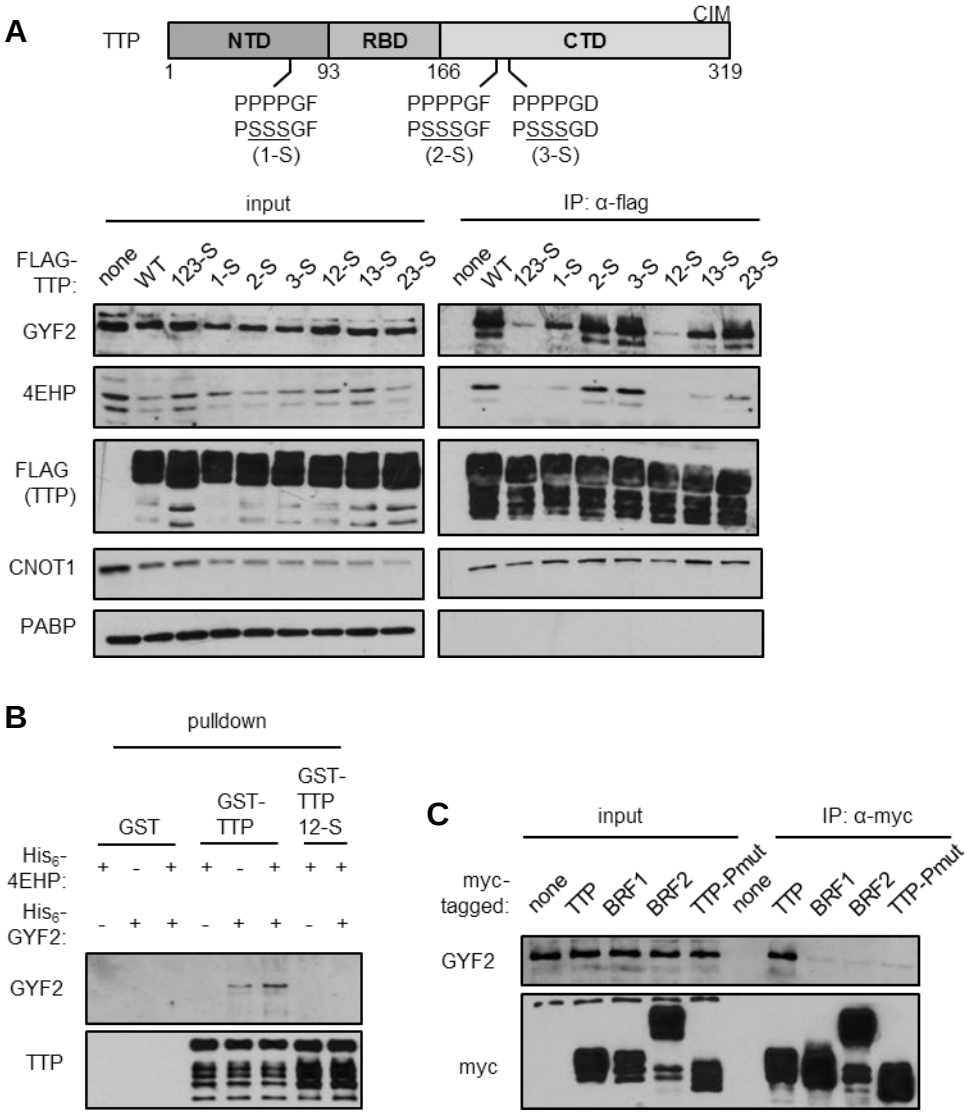

Figure 2.8. TTP interacts with GYF2 through tetraproline motifs 1 and 2. (A) Same as Figure 2.7 panel B, with each of the three tetraproline motifs of FLAG-tagged TTP mutated as indicated in the schematic above (1-S, 2-S, 3-S), and all combinations of those mutations. **(B)** Western blot for an *in vitro* pulldown assays similar to Figure 2.1C, with the addition of GST-tagged 12-S mutant of TTP. **(C)** Western blots of input and anti-myc IP samples from RNase A-treated extracts of HEK293T cells transiently expressing myc-tagged mouse TTP, BRF1 or BRF2. A mutant version of mouse TTP with all prolines of the first tetraproline motif and the immediate downstream four prolines replaced with alanines (Pmut) was also included.

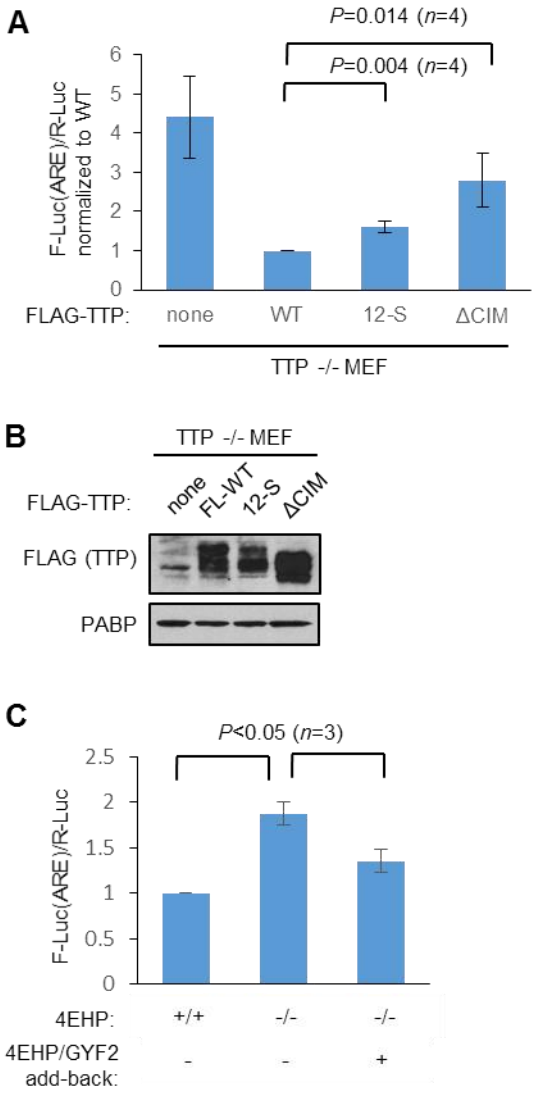

Figure 2.9. TTP mutated in tetraprolines 1 and 2 is impaired in its ability to repress a luciferase reporter ARE-mRNA. (A) Luciferase luminescence assays from TTP$^{-/-}$ MEFs transiently co-expressing wild-type or mutant TTP with two reporters, one encoding firefly luciferase (F-Luc) containing in its 3'UTR the AU-rich element (ARE) from human GM-CSF mRNA, and one encoding *Renilla* luciferase (R-Luc) without an ARE as an internal control. For each sample, F-Luc activity was normalized to R-Luc and values were normalized to the wild-type TTP-transfected condition, which was set as 1. Error bars represent standard error of the mean (SEM) (n = 4). P-values were calculated using Student's t-test (paired, two-tailed). **(B)** Representative western blot of samples used in panel A. PABP was used as the loading control. **(C)** Luciferase assays in 4EHP$^{+/+}$ and 4EHP$^{-/-}$ MEFs similar to the experiment in panel A except in the absence of co-transfected TTP. The experiment on the right was performed in the presence of transiently expressed 4EHP and GYF2. Error bars represent SEM (n = 3).

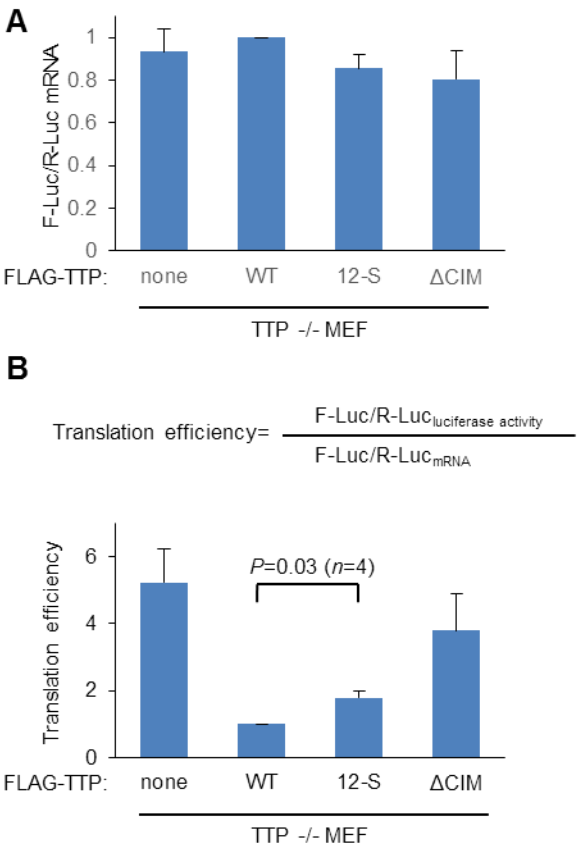

Figure 2.10. Evidence that TTP-mediated repression of the luciferase ARE-reporter mRNA occurs at the level of translation. (A) Levels of firefly luciferase mRNA normalized to *Renilla* luciferase mRNA quantified by qRT-PCR from samples in Figure 2.9A. Error bars represent SEM (n = 4). **(B)** Translation efficiency calculated as ratios of luciferase luminescence over mRNA levels as listed in the shown formula. Error bars represent SEM (n = 4).

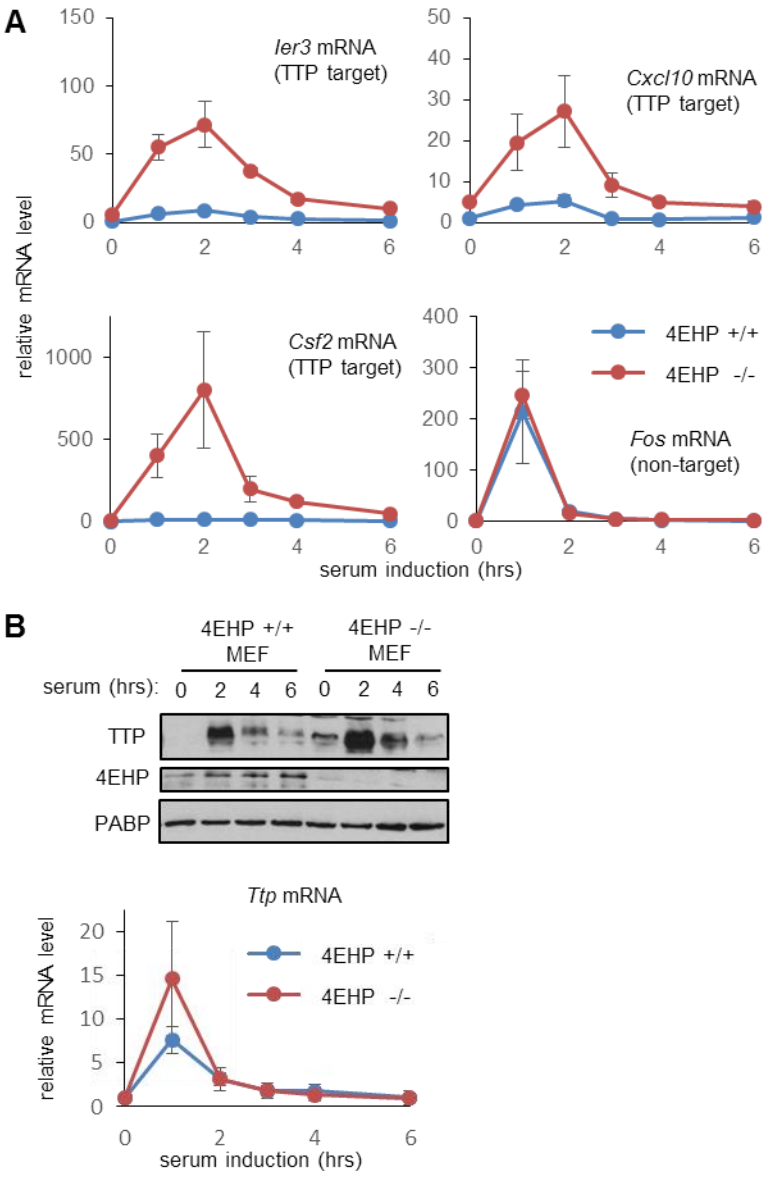

Figure 2.11. 4EHP knockout MEFs show increased induction of TTP target mRNAs. (A) Quantitative qRT-PCR quantification of *Ier3*, *Cxcl10*, *Csf2* and *Fos* mRNA levels during serum induction of MEFs from $4EHP^{+/+}$ (blue) and $4EHP^{-/-}$ (red) littermates. GAPDH mRNA was used as an internal control for normalization and values were normalized to the values for $4EHP^{+/+}$ MEFs at t=0. Error bars represent SEM (n = 3). **(B)** Top: Western blots for TTP, 4EHP and PABP during the serum induction time course described in panel A. Bottom: qRT-PCR quantification of *Ttp* mRNA levels during the serum induction time course with error bars as in panel A.

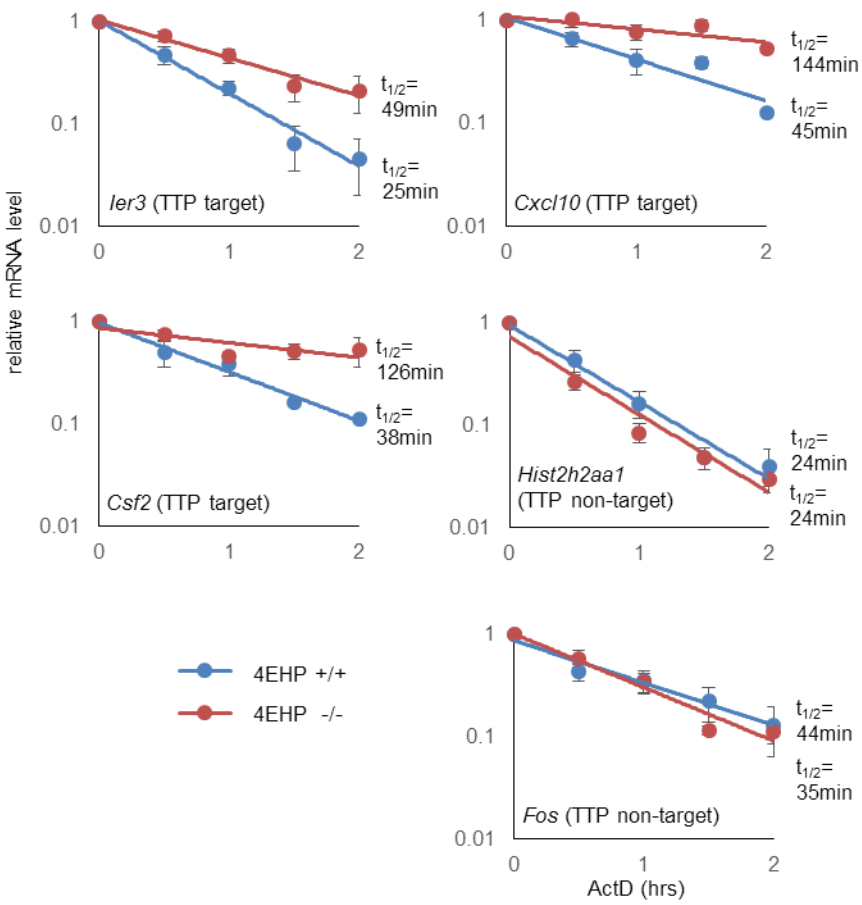

Figure 2.12. 4EHP knockout MEFs show increased stability of TTP target mRNAs. Decay assays using Actinomycin D transcriptional shutoff. mRNA levels were quantified by qRT-PCR and normalized to GAPDH mRNA, with values at t=0 set to 1. Error bars represent SEM (*n* = 3). Calculated half-lives of each mRNA species (assuming an infinite GAPDH mRNA half-life) are listed in minutes.

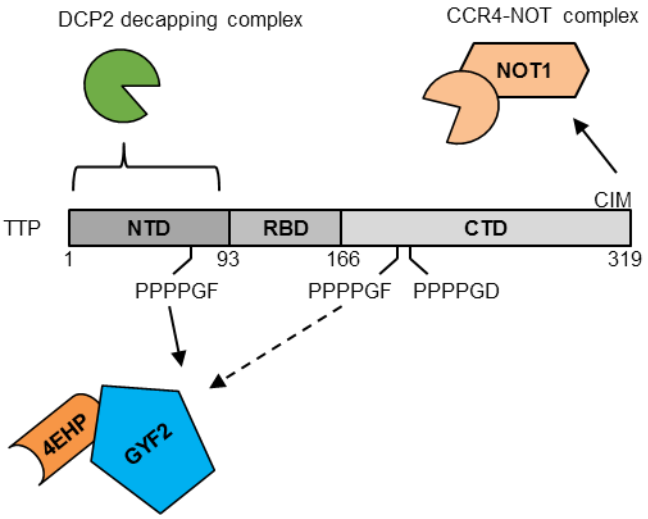

Figure 2.13. TTP recruits multiple co-repressors to repress target mRNAs. Schematic showing TTP motifs and domains contributing to mRNA repression. The CIM recruits the CCR4-NOT deadenylation complex via direct interaction with CNOT1. The NTD of TTP associates with the DCP2 decapping complex. Our work demonstrates the conserved tetraproline motifs of TTP recruiting the 4EHP-GYF2 complex.

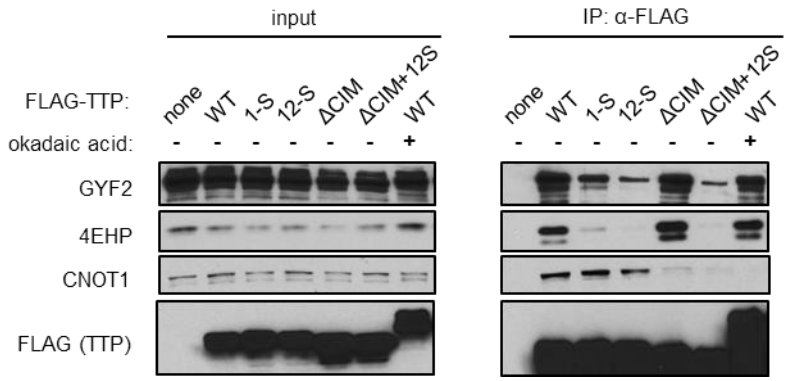

Figure 2.14. Okadaic acid inhibits TTP association with the CCR4-NOT deadenylase complex but not with 4EHP-GYF2. Western blots of total and anti-FLAG IP samples from RNase A-treated extracts of HEK293T cells transiently expressing indicated FLAG-tagged TTP variants, with or without a 2 hour 1 μM okadaic acid (Calbiochem) treatment.

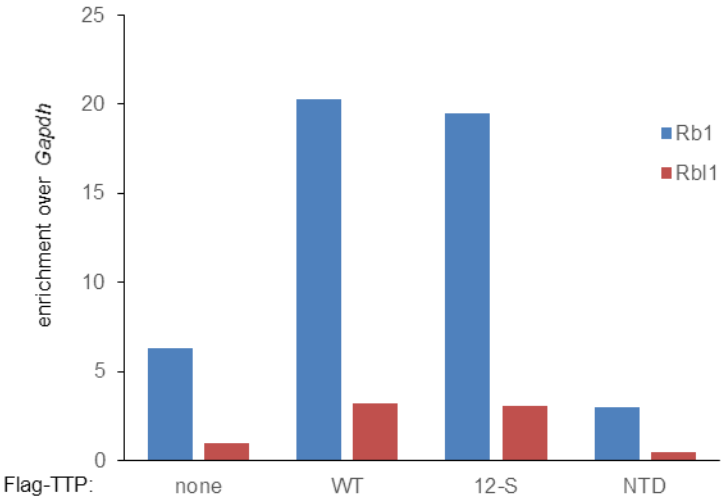

Figure 2.15. Tetroproline-mutant TTP is not deficient in target mRNA binding. Enrichment of Rb1 and Rbl1 mRNAs fold over Gapdh in RNA-IP with the indicated TTP constructed transfected. Relative mRNA levels of input and anti-FLAG RNA-IP were measured by qRT-PCR.

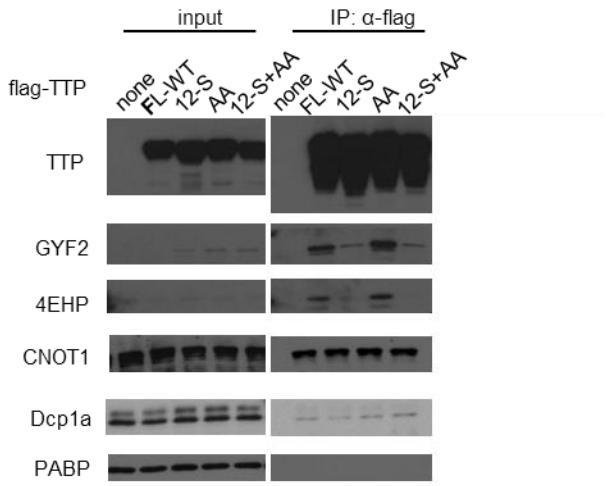

Figure 2.16. Tetraproline-mutant TTP is not deficient in CNOT1 and Dcp1a association. Western blots for indicated factors in input and anti-FLAG IP fractions from RNase A-treated extracts of HEK293T cells transiently expressing indicated FLAG-tagged TTP variants.

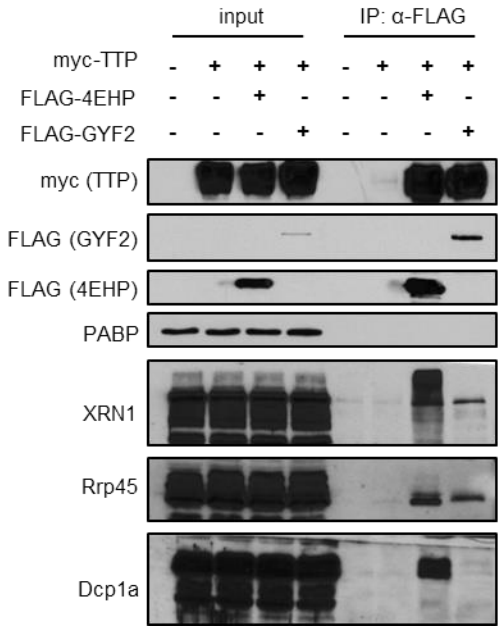

Figure 2.17. 4EHP and GYF2 associate with degradation machinery. Additional western blots detecting degradation factors from the experiment in Figure 2.1C.

2.5 Materials and Methods

Plasmid constructs

Coding sequences (CDS) of mouse TTP, BRF1, BRF2, 4EHP and GYF2 were amplified from cDNA reverse-transcribed using Superscript II (Invitrogen) from total RNA of NIH/3T3 cells, and inserted into pcDNA3-based mammalian expression vectors pcDNA3-myc and pcDNA3-FLAG (79) and bacterial expression vectors pET-his (80) and pGEX-4T1 (Amersham). Sequences encoding domain truncations of TTP were inserted into pcFLAG-NMS2 (80), which fused the domains with MS2 coat protein to add additional size. Firefly luciferase and *Renilla* luciferase CDS were subcloned from pGL2 and pRL (Promega), respectively, into pcDNA3-myc. A 62-bp AU-rich element of human GM-CSF (81) was inserted into the 3'UTR of pcDNA3-myc-Luc. Plasmid sequences are available upon request.

Cell culture

RAW264.7 cells and HEK 293T cells were cultured in Dulbecco's Modified Eagle's Medium (DMEM; Gibco) with 10% fetal bovine serum (FBS). Mouse embryonic fibroblasts were cultured in DMEM containing 1 mM sodium pyruvate (Gibco) with 10% FBS and 2 mM L-Glutamine (Gibco). In experiments in Figure 2.11 and 2.12, cells were washed 2 times with PBS, and grown in DMEM containing 0.5% FBS for a 24 hour serum starvation period. Cells were then serum-induced with DMEM containing 10% FBS for indicated amounts of time. In mRNA decay assays (Figure 2.12), 2 hours after serum induction 10 μg/ml Actinomycin D was added to stop transcription. The decay time course was started after 35 minutes, and samples were harvested into Trizol at indicated time-points.

Antibodies and western blotting

Western blots were performed with the following antibodies at the indicated concentrations: rabbit polyclonal anti-Myc (Sigma-Aldrich, C3956; 1:1,000), rabbit polyclonal anti-FLAG (Sigma-Aldrich, F7425; 1:1000), rabbit polyclonal anti-TTP (Sigma-Aldrich, T5327; 1:500), rabbit polyclonal anti-PABP (Abcam, ab21060; 1:1000), rabbit polyclonal anti-CNOT1 (Proteintech, 14276-1-AP; 1:200), rabbit polyclonal anti-GIGYF2 (Santa Cruz, sc-134708; 1:50), rabbit polyclonal anti-EIF4E2 (GeneTex, GTX103977; 1:200), mouse monoclonal anti-GST (Abgent, AM1011a; 1:600).

Co-immunoprecipitation assays

For co-immunoprecipitation assays, cells in 10cm plates were transfected with 5 µg of the indicated 4EHP, GYF2, TTP, BRF1 or BRF2 constructs, using TransIT 293 reagent according to manufacturer's protocol (Mirus). After 48 hours, cells were washed with PBS, pelleted by centrifugation at 1000 *g* for 5 min, and lysed in 1 ml of ice-cold hypotonic gentle lysis buffer (10 mM Tris-HCl pH 7.5, 10 mM NaCl, 2 mM EDTA, 0.5% Triton-X100, 1 mM PMSF, 1 µM aprotinin, 1 µM leupeptin). Lysates were incubated on ice with 50 µg/ml RNase A for 10 min, and then the NaCl concentration was increased to 150 mM and incubated for another 10 min on ice. The supernatant was separated from debris by centrifugation at 4˚C and 21130 *g* for 15 minutes, and added to 50 µl of anti-FLAG M2-agarose (Sigma) or anti-cMyc agarose (Sigma). Beads were washed 8 times with 1ml NET2 (50 mM Tris-HCl pH 7.5, 150 mM NaCl, 0.05% Triton-X100), and resuspended in 50 ul 2x SDS loading buffer (100 mM Tris-HCl pH 6.8, 4% SDS, 20% glycerol, 0.1% bromophenol blue, and 200 mM DTT) for separation by SDS-polyacrylamide gel electrophoresis (PAGE) and Western blotting using standard procedures.

TTP-IP and Liquid chromatography/tandem mass spectrometry (LC/MS-MS)

24 µg of rabbit anti-TTP (Sigma-Aldrich, T5327) or normal rabbit serum were incubated with 50 mg of protein A Sepharose CL-4B beads (Fisher) overnight in 1.2 ml NET2. RAW264.7 cell were treated with 100 ng/ml of lipopolysaccharides (LPS) for indicated lengths of time (0, 2, 4, 8 or 24 hours). For each time point, 3 15-cm plates of cells were lysed with 4 ml hypotonic gentle lysis buffer, treated with RNase A and adjusted to 150 mM NaCl as described above for co-immunoprecipitation assays, added to protein A Sepharose-coupled antibodies and washed. Beads were then eluted 3 times with 500 µl 0.1 M glycine pH 2.6. Eluants were pooled and mixed with 20% Trichloroacetic acid (TCA) at -20˚C overnight. After thawing on ice, protein samples were centrifuged at 21130 *g* for 30 min at 4˚C. Pellets were then washed with 10% TCA and 3 times -20˚C pre-chilled acetone, spinning at 4˚C 21130 *g* for 15 min in between washes. Pellets were air-dried and stored at -80˚C. LC/MS-MS was performed as described previously (82).

Bacterial protein purification and *in vitro* pull-down assays

For bacterial expression of mouse TTP, GYF2 and 4EHP, corresponding pET-his or pGEX-4T1 plasmids were transformed into *E. coli* BL21(DE3) cells containing the pRI952 plasmid encoding rare arginine and isoleucine tRNAs (83). Bacteria were cultured in 200 ml LB broth medium at 37˚C to OD_{600} of 0.5, and then transferred to lower temperature and induced with isopropyl β-D-1-thiogalactopyranoside (IPTG). IPTG concentration, temperature and time of incubation differed for individual proteins as follows: GST: 0.1 mM IPTG, 15˚C, 16 hours; GST-TTP: 0.3 mM IPTG, 25˚C, 3 hours; GST-TTP-12S: 0.1 mM IPTG, 15˚C, 16 hours; His_6-GYF2: 0.4 mM IPTG, 15˚C, 8 hours;

His_6-4EHP: 0.1 mM IPTG, 15˚C, 16 hours. Cells were pelleted at 2300 *g* for 10 minutes, resuspended in 5 ml TKET buffer (10 mM Tris-HCl pH7,5, 100 mM KCl, 0.1 mM EDTA, 0.05% Triton X100) with 1 mM PMSF, sonicated at 4˚C for 8 x 30 seconds, with 30 second intervals, added Triton X100 to 0.5%, nutated for 15 min, and centrifuged at 11000 *g* for 15 minutes to remove debris. Supernatant was then allowed to flow through columns of 700 µl glutothinone Sepharose 4B (GE) or 700 µl Ni-NTA agarose beads (Qiagen) twice. Columns were then washed 3 times with 4 ml of TKET, and eluted with 500 µl of Tris-HCl pH 7.5 with 100 mM KCl and 20 mM glutathione for GST proteins or 500 µl of TKET containg 200 mM imidazole for His_6-4EHP. Elutants were dialyzed overnight at 4˚C against 400 ml of PBS, and protein concentration was measured using a Bradford-based Bio-Rad Protein Assay system and freshly-made bovine serum albumin (BSA) standards. His_6-GYF2 was purified under denaturing conditions, following the same steps, except: lysis buffer is changed to TKET containing 1mM PMSF, 20 mM imidazole and 6 M Guanidine-HCl; cells were incubated at room temperature for 30 min for lysis instead of sonication; wash buffer is changed to TKET containing 8 M urea and 20 mM imidazole; elution buffer is changed to TKET containing 8 M urea and 200 mM imidazole

For *in vitro* pull-down assays, 5 µg His_6-GST or GST-TTP were nutated with 25 µl of glutathione Sepharose for 2 hours at 4˚C, washed 3 times with TKET, and then nutated with 5 µg of His_6-4EHP and/or His_6-GYF2 in 500 µl TKET at 4˚C. After 2 hours, beads were washed 4 times with 700 µl TKET, and resuspended in 2x SDS loading buffer, to be analyzed by SDS-PAGE and western blotting.

Luciferase assays

MEFs were plated at ≈20% confluency in 22-mm diameter tissue culture wells in 1 ml DMEM/10%FBS. 24 hours later, 0.2 µg pcDNA3-myc-F-Luc-ARE, 0.05 µg pcDNA3-myc-R-Luc, 0.3 µg pSuper.puro (OligoEngine), 0.4 µg pcDNA3-myc, and 0.05 µg of FLAG-tagged TTP wild-type or mutant constructs were transfected by TransIT-X2 following manufacturer's protocols (Mirus). 24 hours later, 5 µg/ml of puromycin was added for another 24 hours to select for transfected cells. Cells were then lysed in 250 µl of 1x Passive Lysis Buffer (Promega) for 20 minutes at room temperature and 10 µl of each lysate was assayed for firefly and *Renilla* luciferase activities using Dual-Luciferase Reporter Assay (Promega) reagents in a NOVOstar microplate reader. In the experiments in Figure 2.9C, 0.3 µg of pcDNA3-FLAG or 0.15 µg pcDNA3-FLAG-4EHP and 0.15 µg pcDNA3-FLAG-GYF2 were co-transfected instead of TTP constructs. *P*-values were calculated with two-tailed paired Student's *t*-test.

Quantitative qRT-PCR

3 µg of total RNA prepared from cells using Trizol (Invitrogen) was treated with 0.1 U/µl DNase I (Invitrogen AM2222) in 20 µl RNase-free H_2O (Ambion) with 2 U/µl RNaseOUT (Invitrogen) at 37°C for 30 min. RNA was subsequently extracted with Phenol:Chloroform:Isoamyl alcohol (50:49:1), ethanol precipitated, washed with 70% ethanol and dissolved in 15 µl of RNase-free H_2O. 1 µg of the DNase-treated RNA was reversed transcribed using random hexamers with Superscript III according to manufacturer's protocols (Invitrogen). The corresponding cDNA was used for qPCR quantification using Fast SYBR Green Master Mix (Applied Biosystems) on a StepOnePlus System (Applied Biosystems). Each cDNA-primer set was measured in duplicates. For each qRT-PCR reaction, 5-fold serial dilutions of cDNA were used to calculate PCR efficiency (E) and standard curve of log10 of dilution factor vs Ct

(threshold cycle) was plotted to determine the linear range of Ct values. For E ranged between 1.8 and 2.1, and Ct within the linear range, relative mRNA levels were calucated with the formula: $E^{\wedge-\Delta Ct}$. Non-RT controls were monitored to confirm DNase treatment was complete.

The following DNA oligos were used (at 285 nM and 58°C annealing temperature, melting curves for each set is monitored to avoid multiple products) F-Luc_F: CTT CGC CAA AAG CAC TCT G; F-Luc_R: GAG CCC ATA TCC TTG TCG TAT C; R-Luc_F: TGG AGC CAT TCA AGG AGA AG; R-Luc_R: TGT AGT TGC GGA CAA TCT GG; TTP-F: CGG AGG ACT TTG GAA CAT AAA C; TTP-R: GGA GTT GCA GTA GGC GAA GTA G; GAPDH_F: CAT GGC CTT CCG TGT TCC TA; GAPDH_R: CCT GCT TCA CCA CCT TCT TGA T; IER3_F: GCG CGT TTG AAC ACT TCT C; IER3_R: CAG AAG ATG ATG GCG AAC AG; CXCL10_F: CTA GCT CAG GCT CGT CAG TTC; CXCL10_R: TGG GAA GAT GGT GGT TAA GTT C; CSF2_F: TGA ACA TGA CAG CCA GCT ACT AC; CSF2_R: ACT TGT GTT TCA CAG TCC GTT TC; FOS_F: GAA TGG TGA AGA CCG TGT CAG ; FOS_R: GTC TCC GCT TGG AGT GTA TC; HIST2H2AA_F: AAG CTG CTG GGC AAA GTG; HIST2H2AA_R: ACT TGC CCT TCG CCT TAT G.

2.6 Acknowledgments

Chapter 2, in full, has been submitted for publication of the material as Fu R., Olsen M., Webb K., Bennett E., Lykke-Andersen J. The dissertation author was the primary investigator and author of this material.

Chapter 3. TTP family proteins regulate the stability of retinoblastoma protein mRNAs during serum-stimulated G_0-S transition

3.1 Introduction

The eukaryotic cell cycle is under tight regulation to control cell proliferation (84). A mutational hotspot for oncogenesis, the G_1 checkpoint serves as a point of cell cycle commitment. Passage through this checkpoint allows progression into the S phase, where DNA synthesis occurs (85). The CDK-RB-E2F pathway plays an important role in regulating the G_0-G_1-S cell cycle transition by controlling the transcription of factors required for DNA synthesis and cell cycle progression (86).

The retinoblastoma (Rb*)* family of proteins play a central role in the CDK-RB-E2F pathway by controlling the activity of E2F transcription factors (87). In the G_0 or early G_1 phase of the cell cycle, E2F transcription factors are bound and repressed by Rb proteins RB1, RBL1 and RBL2 (88-91). Activation of cyclin-CDK pairs CDK4/6-Cyclin D1 and CDK2-Cyclin E results in phosphorylation of Rb family proteins (92), causing activation of E2F factors and transcription of E2F target genes, which promotes cell cycle progression into S-phase (93, 94). The Rb family display dynamic changes in protein levels during G_0-G_1-S transition (95). Interestingly, the half-life of *Rbl2* mRNA was previously found to undergo a dramatic change as cells transition into proliferation from a quiescent state during T cell activation (96), suggesting that *Rb* family mRNAs and the CDK-RB-E2F pathway could be regulated at the mRNA decay level in addition to the well described regulation at the protein level.

The TTP family of zinc-finger proteins, consisting of TTP, BRF1 and BRF2, are mRNA decay-activating RNA-binding proteins that recognize mRNAs with 3'UTR AU-rich elements (15, 63, 64). Of the three, TTP is the most studied, and has been demonstrated to regulate turnover of a variety of mRNAs, including mRNAs encoding

cytokines during the immune response (16, 17, 54). BRF1 and BRF2 contain zinc finger motifs responsible for RNA binding that are highly similar to that found in TTP, and like TTP are capable of recruiting decay machinery to bound mRNAs (17, 54, 55). However, the target mRNAs for BRF1 and BRF2 are less well described.

Here we show that the TTP family proteins display different expression patterns during serum-mediated induction of the G_0-G_1-S transition in mouse embryonic fibroblasts. TTP and BRF1 associate with Rb family mRNAs, which contain conserved AU-rich elements. Furthermore, knockdown of TTP proteins leads to stabilization of Rb family mRNAs, lowered E2F downstream target transcription, and a modest delay in G_0-G_1-S transition. These observations suggest a role for TTP family proteins in facilitating the cell cycle.

3.2 Results

TTP family proteins are differentially regulated by serum induction

To compare the behavior of TTP family proteins during serum activation in fibroblasts, we deprived NIH3T3 mouse fibroblasts of serum for 48 hours to cause exit from the cell cycle into the quiescent G_0 stage, followed by cell cycle activation with 20% serum (Figure 3.1). Compared to cycling cells, arrested cells were depleted for BRF1, whereas BRF2 accumulated at slightly increased levels (Figure 3.2A). Consistent with previous reports (62), TTP was rapidly upregulated upon serum activation, peaking around 1.5-3 hours after stimulation. This upregulation was coupled with migration shifts toward higher molecular weight in SDS-PAGE gels, consistent with the concurrence of post-translational modifications (22-24, 61). We observed a similar, but less dramatic induction for BRF1, whereas BRF2 levels initially decreased, before increasing at later time-points when TTP and BRF1 protein levels started to decrease.

Quantification of mRNA levels by qRT-PCR revealed patterns of mRNA induction that mirrored those of the corresponding proteins (Figure 3.2B), suggesting that much of the regulation occurs at the transcript level.

Rb family mRNAs associate with TTP proteins

Retinoblastoma proteins play a critical role in the G_0-G_1-S cell cycle transition. Analysis by AREsite and AREscore prediction algorithms (8, 97) predicted 3'UTR AREs in mRNAs encoding retinoblastoma proteins (Table 3.1). Consistent with this, *Rb1 and Rbl2* mRNAs have been found in previously published datasets for mRNAs enriched in co-immunoprecipitation with the AUBPs HuR and BRF2, respectively (32, 98). This raised the possibility that mRNAs for Rb factors are targeted by TTP proteins to facilitate cell cycle progression.

To test this idea, RNA-immunoprecipitation assays were conducted to monitor for association of TTP family proteins with *Rb* family mRNAs in serum-stimulated NIH 3T3 cells. *Rb1*, *Rbl1*, and *Rbl2* mRNAs were observed to co-purify with antibodies against TTP and BRF1, with maximal co-purification observed after 3 hours of serum stimulation, correlating with the peak in TTP and BRF1 expression (Figure 3.3). *Mmp13* mRNA, a previously reported target of TTP (99), served as a positive control. We failed to achieve satisfactory immunoprecipitation for BRF2.

Rb mRNAs are targeted for degradation by TTP proteins

We next monitored whether half-lives of *Rb1*, *Rbl1* and *Rbl2* mRNAs were affected by depletion of TTP proteins. Asynchronous NIH/3T3 cells treated with siRNAs targeting TTP family members were incubated with Actinomycin D to inhibit transcription and Rb mRNA levels were measured at different time points by qRT-PCR.

In samples treated with siRNAs targeting all three TTP factors (Figure 3.4A, mRNA decay was markedly impaired for *Rb1, Rbl1* and *Rbl2* mRNAs (Figure 3.4B). By contrast, the half-life of *Fos* mRNA was unaffected under TTP family knockdown conditions, which was expected as TTP family proteins are not limiting for *Fos* mRNA decay (16, 71). Consistent with the stabilization of *Rb1* and *Rbl2* mRNAs, these mRNAs accumulated at higher steady state levels during starvation and 15 hours into serum reactivation in the TTP/BRF1/BRF2 knockdown cells (Figure 3.5).

Downstream transcriptional targets of the CDK-RB-E2F pathway are suppressed by TTP/BRF1/BRF2 knockdown

An overall output of the CDK-RB-E2F pathway is E2F-activated transcription of downstream targets, which in turn stimulate cell cycle-related processes including G_1-S progression (for instance, *Ccne1*), differentiation (*Mybl2*), and DNA replication licensing (*Ttk* and *Mcm6*). We compared the mRNA levels of these E2F targets in the TTP/BRF1/BRF2 knockdown condition (Figure 3.6). Fifteen hours after serum stimulation of starved cells, when S phase markers are detected by western blotting (100), all four monitored target mRNAs were significantly repressed in the siRNA-treated cells (Figure 4). This observation is consistent with the idea that TTP proteins contribute to activation of the CDK-RB-E2F pathway during serum activation.

Depletion of TTP family proteins slows G_0-S progression

Next, the overall effect of the TTP family proteins on G_0-S cell cycle progression was investigated. First, using an assay that monitors total RNA levels to discriminate cells in G_0 from those that are actively cycling (101) categorized over 90% of confluence-arrested 3T3 cells in G_0 in both control and TTP family knockdown conditions (Figure 3.7A). As compared to the control, knockdown of TTP did not

significantly alter the fraction of cells entering the cell cycle after 24 hours of serum stimulation as monitored by RNA content. By contrast, a modest, but statistically significant, decrease in the fraction of cells entering the cell cycle as measured by this assay was observed for cells treated with siRNAs against BRF1, BRF2 and all three TTP family members together (Figure 3.7B). This effect was similar to that seen with an siRNA targeting Cyclin D, suggesting that cell cycle progression was delayed.

A complementary approach, which uses immunofluorescence to monitor the percentage of cells staining for Ki-67, a proliferation marker highly expressed in proliferating but not quiescent cells (102), also revealed defects in cell cycle entry after starvation-induced G_0 arrest upon knockdown of BRF1 and/or BRF2 (Figure 3.8). Collectively, our observations suggest that TTP family proteins promote degradation of *Rb* family mRNAs during the G_0-G_1-S phase transition of the cell cycle, contributing to increased transcription of E2F targets and promotion of cell cycle entry.

3.3 Discussion

We have characterized the induction of TTP family proteins during serum-induced G_0-G_1-S cell cycle transition, and their effect on the CDK-RB-E2F pathway in mouse embryonic fibroblasts. We identify mRNAs encoding Rb proteins RB1, RBL1 and RBL2 as targets of the TTP family. These mRNAs were stabilized upon siRNA-mediated knockdown of TTP proteins (Figure 3.4), and were enriched in IPs for TTP and BRF1 (Figure 3.3). E2F transcription targets *Ccne1*, *Mybl2*, *Ttk* and *Mcm6,* all factors playing important roles in the G_1 and S phase transition, were repressed upon siRNA knockdown of TTP/BRF1/BRF2 (Figure 3.5). Thus, Rb proteins, which are known to be rapidly repressed at the protein level upon cell cycle activation, are also

regulated at the mRNA turnover level, which helps facilitate proper de-repression of E2F transcription activation.

We observed very distinct expression patterns of TTP, BRF1, and BRF2 during serum starvation and stimulation. This raises the question how each gene is differentially regulated for expression. The rapid induction of TTP and BRF1, and the initial decrease of BRF2 after serum addition is observed at the mRNA level, suggesting changes in transcription or mRNA decay, In particular, TTP, BRF1 and BRF2 very likely regulate each other, since AU-rich elements are found in the 3'UTR of all 3 genes. To support this, siRNAs against one gene is often observed to increase the protein level of another. The delayed increase of BRF2 protein, however, cannot be explained by the regulation at the mRNA level alone; translation or protein stability regulation of BRF2 is very likely. Notably, all three proteins shift in migration pattern through the time course, suggesting post-translational modifications that may impact their activity. Whether differential regulations of TTP, BRF1 and BRF2 are required for correct regulation of specific ARE-containing mRNAs remains an intriguing question.

Our work implicates TTP, BRF1 and BRF2 in cell cycle regulations through regulating decay of ARE-containing mRNAs. This supports the notion that ARE-mediated decay is involved in cell cycle control, in conjunction with previous reports of another ARE-binding protein HuR regulating proliferation in colorectal carcinoma cells (103). In the early hours of serum stimulation after starvation, the RNA-stabilizing HuR is localized to the nucleus, presumable unable to compete with rapidly induced TTP and BRF1 for target binding. As the cell cycle progresses, the timing of HuR transport to the cytoplasm coincides with the decrease of TTP and BRF1 protein levels. This illustrates a coordination at multiple levels to regulate ARE-mRNAs.

3.4 Figures and Tables

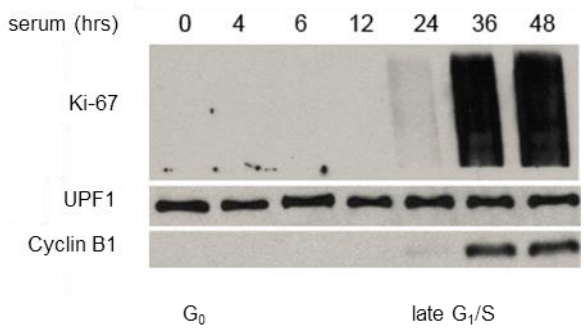

Figure 3.1. Arrested 3T3 cells transition into S phase around 24 hr after serum induction. Western blot for Ki-67 and Cyclin B1 in 3T3 cells serum stimulated for the indicated lengths of time. UPF1 was used as an internal control.

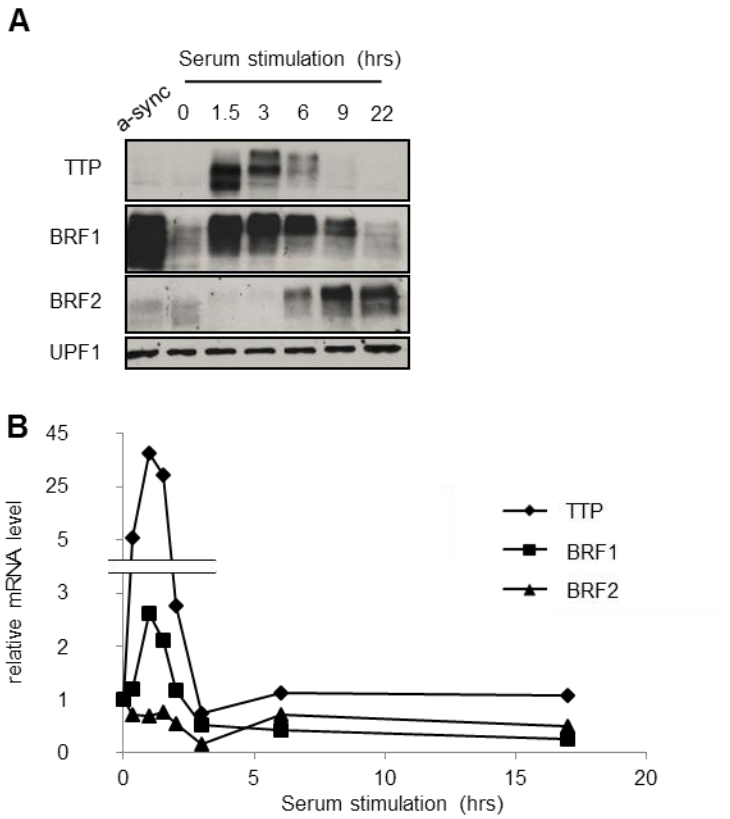

Figure 3.2. TTP family proteins are differentially induced during serum induced G_0-G_1-S transition. (**A**) Western blot for 3T3 cells induced after 48 hr of serum starvation by 20% FBS, for indicated amounts of time. UPF1 was used as a loading control. (**B**) qRT-PCR quantification of TTP family mRNA levels in the serum induction time course.

Table 3.1. mRNAs encoding retinoblastoma proteins are predicted to contain AU-rich elements. The number of AUUUA pentamers in human mRNAs, and the number of which were conserved to mouse, were retrieved from ARE site database query. ARE score calculated the likelihood of mouse 3'UTRs being targeted by ARE-mediated decay. Median ARE score of the mouse transcriptome is 1.3.

	ARE site, *Gruber, et al*		ARE score, *Spasic, et al*
	AUUUA	Conserved	ARE score
Rb1	11	8	14.3
Rbl1	4	1	5.2
Rbl2	5	2	5.9

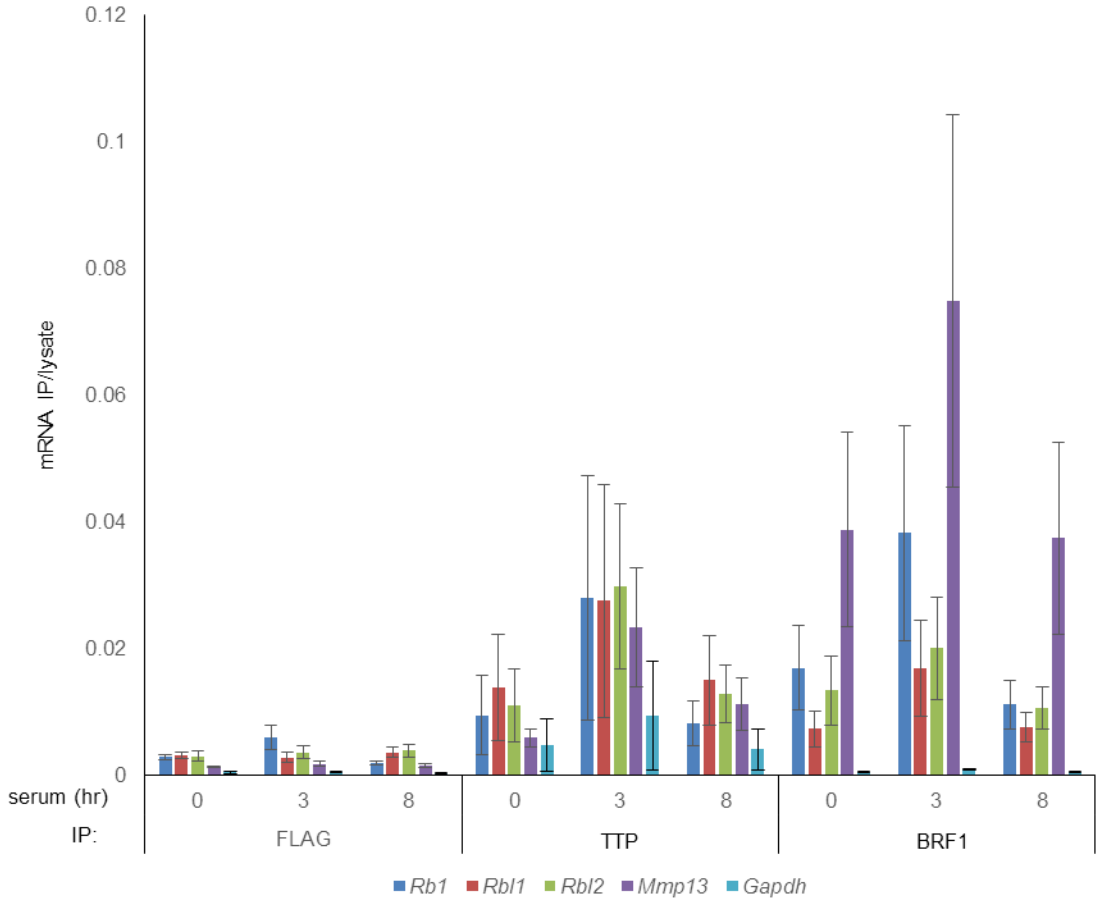

Figure 3.3. Rb family mRNAs associate with TTP and BRF1. qRT-PCR quantification of RNA co-immunoprecipitating from NIH3T3 cells with antibodies against TTP and BRF1. Anti-FLAG was used as a negative control. Cells were harvested at the indicated time points after serum induction. Fractions of IP-recovered was calculated as compared to the lysate mRNA levels. *Mmp13* was previously identified to interact with TTP. Error bars represent Standard Error of the Means (SEM) (n = 4).

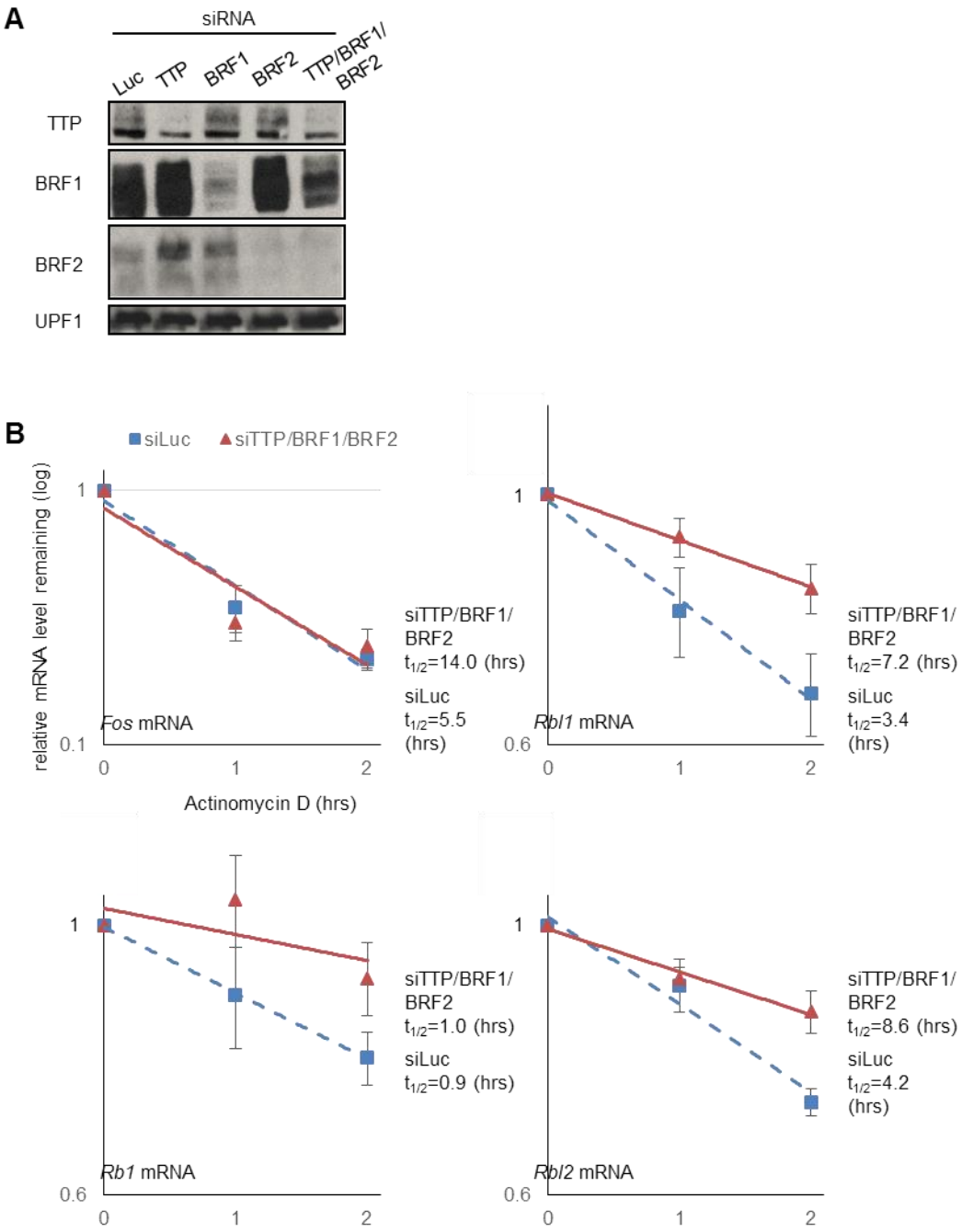

Figure 3.4. Knockdown of TTP family proteins stabilizes *Rb1*, *Rbl1* and *Rbl2* mRNAs. (**A**) Western blot of 3T3 cells treated with the indicted siRNAs. UPF1 was used as an internal control. (**B**) qRT-PCR quantification of Actinomycin D-mediated mRNA decay assays. *Gapdh* was used as an internal control. Relative mRNA levels were normalized to the 0 hr time point, set as 1. *Fos* mRNA was used as a control not affected by loss of TTP family proteins. Half-lives were calculated assuming *Gapdh* is infinitely stable through the time course.

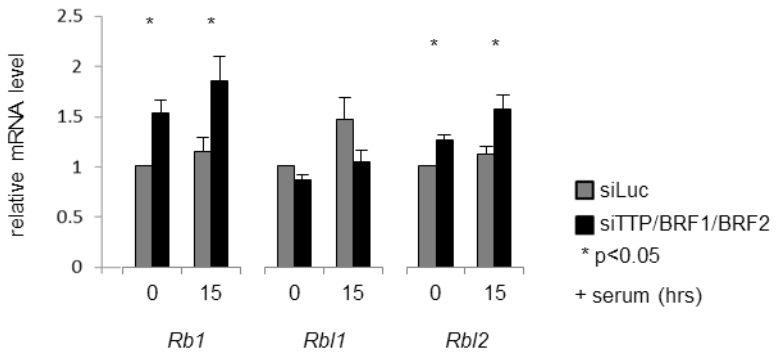

Figure 3.5. *Rb1* and *Rbl2* mRNA levels are elevated in NIH 3T3 cells treated with siRNAs against the TTP family proteins. qRT-PCR quantification of Rb family mRNAs treated with siRNAs against luciferase or TTP family genes. Relative mRNA levels were normalized to internal control *Gapdh* mRNA, with mRNA levels of the siLuc 0 hr condition set as 1. Error bars represent SEM (n = 3). P values were calculated by paired 2-tailed Student's t-test. * represent P<0.05.

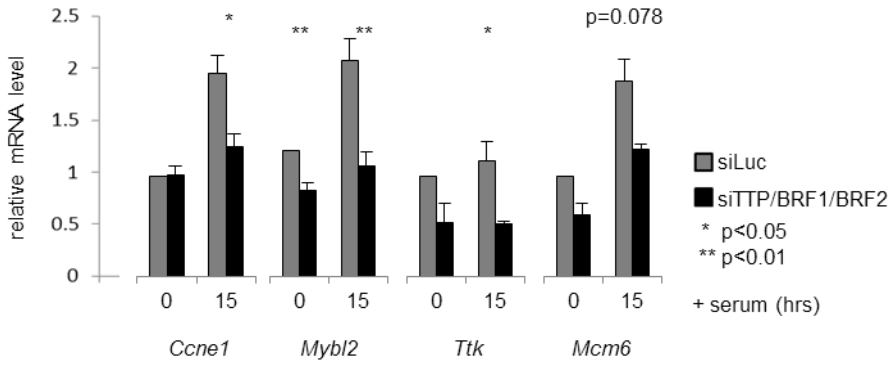

Figure 3.6. Knockdown of TTP family proteins represses E2F target transcription. qRT-PCR quantification of E2F target mRNA levels at before and 15 hr after serum induction. Relative mRNA levels were normalized to *Gapdh* mRNA as the internal control, with mRNA levels of the siLuc 0 hr condition set as 1. Error bars represent SEM (n = 4). P values were calculated by paired 2-tailed Student's t-test. * and ** represent $P<0.05$ and $P<0.01$, respectively.

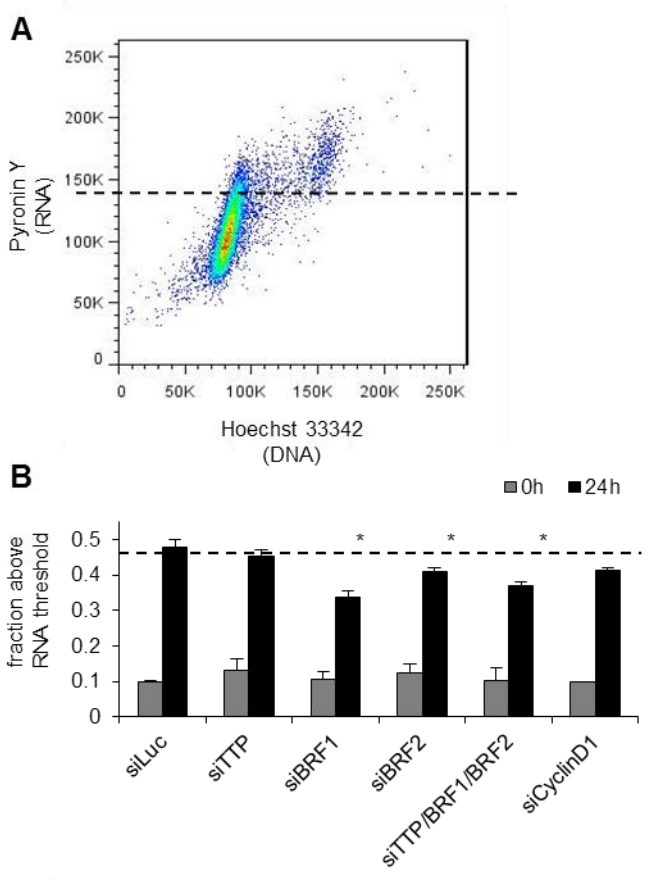

Figure 3.7. Deficiencies in TTP family proteins slow G_0-G_1-S transition. (**A**) Flow cytometry analysis of starved cells stained by Hoechst 33342-PY. RNA content threshold is set at the lowest RNA content of G_2 cells, which was identified by double DNA content. (**B**) Fraction of cells above RNA threshold before and 24 hr after serum induction. RNA content of cells was monitored by flow cytometry. RNA threshold was set to the lowest RNA content of S-phase cells. Error bars represent SEM (*n* = 3). *P* values were calculated by paired 2-tailed Student's *t*-test. * represent *P*<0.05.

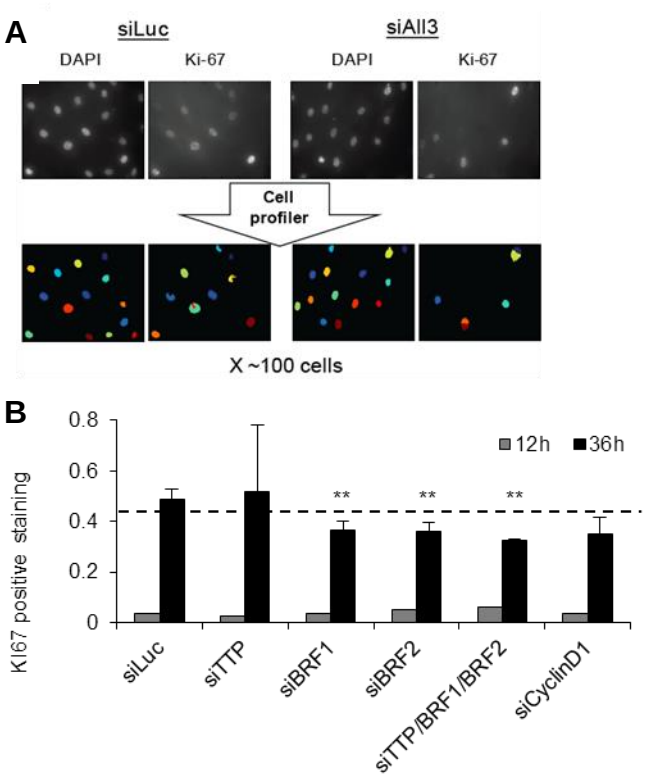

Figure 3.8. Deficiencies in TTP family proteins slow exit from quiescence. (**A**) Immunofluorescence imaging and CellProfiler processing for Ki-67 positive staining. (**B**) Fraction of cells positive for Ki-67 staining at 12 and 36 hr serum induction. ~100 cells were randomly imaged by immuofluoresence for each siRNA condition per repeat. Cell outlines and Ki-67 positive cell count were generated by CellProfiler program. Error bars represent SEM (n = 3). P values were calculated by paired 2-tailed Student's t-test. * and ** represent P<0.05 and P<0.01, respectively.

3.5 Materials and Methods

Cell culture

NIH 3T3 Tet-Off cells (Clontech) were cultured in Dulbecco's Modified Eagle's Medium (DMEM; Gibco) with 10% fetal bovine serum (FBS). For starvation arrest, cells were washed 2 times with PBS, and grown in DMEM containing 0.5% FBS for 48 hours. Cells were then serum induced with DMEM containing 20% FBS for indicated amounts of time. In mRNA decay assays, 10 µg/ml Actinomycin D was added to cells to stop transcription. The decay time course was started after 35 minutes, and samples were harvested into Trizol (Invitrogen) at indicated time-pionts and RNA was isolated according to the manufacturer's recommendation.

Antibodies and western blotting

Western blots were performed with the following antibodies at the indicated concentrations: rabbit polyclonal anti-TTP (Sigma-Aldrich, T5327; 1:500), rabbit polyclonal anti-BRF1 (Cell Signaling, 2119; 1:500), rabbit polyclonal anti-BRF2 (Santa Cruz, sc-365908; 1:100), rabbit polyclonal anti-UPF1 ((80);1:1000), rabbit polyclonal anti-Ki67 (Abcam, ab15580; 1:1000), rabbit polyclonal anti-cyclinB1 (Cell Signaling, 4138; 1:1000).

siRNA knockdown

siRNAs were transfected using TransIT-TKO according to the manufacturer's recommendations (Mirus). 60 nM of siLuc (104), siTTP (targeting GAAUCCUGGUGCUCAAAUU), siBRF1 (GUAACAAGAUGCUCAACUA), siBRF2 (CCACAACUCAAUAUGAAAA) and siCyclinD1 (105) were used. For some experiments, siTTP, siBRF1 and siBRF2, 20 nM of each, were combined.

RNA-immunoprecipitation assays

7 µg anti-FLAG, anti-TTP or anti–BRF1 antibody was nutated with 60 µl protein A Sepharose CL-4B beads (Fisher) overnight in 400 µl NET2 (50 mM Tris-HCl pH7.5, 150 mM NaCl, 0.05% Triton-X100). Cells were lysed in 1 ml of ice-cold hypotonic gentle lysis buffer (10 mM Tris-HCl pH7.5, 10mM NaCl, 2 mM EDTA, 0.5% Triton-X100, 1 mM PMSF, 1 µM aprotinin, 1 µM leupeptin, 40 U/ml RNaseOUT). Lysates were incubated ice for 10 min, and then the NaCl concentration was increased to 150 mM, and incubated for another 10 min on ice. The supernatant was separated from debris by centrifugation at 4˚C and 21130 *g* for 15 min, and added to antibody-coupled beads. After nutating for 2 hours, beads were pelleted by 1 min 1000 *g* centrifugation, and washed 8 times with ice-cold NET2. RNA from the beads was then recovered by eluting with 1 ml Trizol (Invitrogen).

Quantitative qRT-PCR

3 µg total RNA isolated with Trizol was treated with 0.1 U/µl DNase I (Invitrogen AM2222) in 20 µl RNase-free H_2O (Ambion) with 2 U/µl RNaseOUT at 37˚C for 30 min. RNA was subsequently extracted with Phenol:Chloroform:Isoamyl alcohol (50:49:1), followed by ethanol precipitation, wash with 70% ethanol, and dissolved in 15 µl RNase-free H_2O. 1 µg of the DNase-treated RNA was reverse transcribed using random hexamers with Supercript III according to manufacturer's protocols (Invitrogen). The corresponding cDNA was used for qPCR quantification using Fast SYBR Green Master Mix on a StepOnePlus System (Applied Biosystems). For each qRT-PCR experiment, 5-fold serial dilutions were used to calculate PCR efficiency (E), and a standard curve of log10 of dilution factor vs Ct (threshold cycle) was plotted to

determine the linear range of Ct values. For E ranges between 1.8 and 2.1, and Ct within the linear range, relative mRNA levels were calculated as $E^{\wedge-\Delta Ct}$. Controls samples treated in the absence of reverse transcriptase were monitored to confirm DNase treatment was complete. The following DNA oligos were used at 285 nM. GAPDH_F: CAT GGC CTT CCG TGT TCC TA; GAPDH_R: CCT GCT TCA CCA CCT TCT TGA T; MMP13_F: ATG AAA CCT GGA CAA GCA GTT C; MMP13_R: AGT GAT CCA GAC CTA GGG AGT G; CFOS_F: GAA TGG TGA AGA CCG TGT CAG ; CFOS_R: GTC TCC GCT TGG AGT GTA TC; TTP_F: CGG AGG ACT TTG GAA CAT AAA C; TTP_R: GGA GTT GCA GTA GGC GAA GTA G; BRF1_F: CCC GAT GGC ACC AAT AAC; BRF1_R: CCC ATG CTA GGA GCA AAG AG; BRF2_F: CCA CAC TTC TGT CAC CCT TCT AC; BRF2_R: TCC CTA CCG CCT TCT TGT C; RB1_F: GAA GAG GCA AAC GTG GTT ACT C; RB1_R: TGT GCC CAA CAT CCT TTA CTC; RBL1_F: TGG AAC ACC TCG AAA GTT CAC; RBL1_R: AAA TAC CGC CGT CCA GTA AG; RBL2_F: GGA AAT GCC CTT CAG TGT TC; RBL2_R: TTT AGA GTC CTT GGG GTG ACA G; CCNE1_F: GGA AAA TCA GAC CAC CCA GAG; CCNE1_R: GAC TTC GCA CAC CTC CAT TAG; MYBL2_F: CAA GAA GGT CCG CAA GTC TC; MYBL2_R: TGA GCA GGC TGT TAC CCT CT; TTK_F: AGA ACT TGC CTC CAC AAG ATG; TTK_R: AAG GGG CAT GAC CGT TTA G; MCM 6_F: TGT CCC GCT TTG ATC TCT TC; MCM6_R: CGC CTG GCA ATA GCA TAA TC.

Flow cytometry

Cells were trypsinized with 0.05% Trypsin-EDTA (Gibco) in PBS, and washed 3 times in 1 ml ice-cold PBS, centrifuging at 1000 *g* for 3 min. Pelleted cells were resuspended in 200 µl PBS with 2 mM EDTA. 600 µl of 70% ethanol was added drop-wise while vortexing. Cells were fixed overnight at 4˚C, and then removed by 1000 *g*

centrifugation at 4˚C for 5 min. Pelleted cells were then washed once and resuspended in 500 µl ice-cold Hanks' balanced salt solution (HBSS). 500 µl Pyronin Y-Hoechst 33342 staining solution (2 mg/l Hoechst 33342, 4 mg/l PY, in HBSS) was added to the cell suspension, and incubated for 20 min at room temperature in the dark. Cells were recorded with LSRII Flow Cytometer (BD) and FACSDiva software (BD). Hoechst 33342 and PY fluorescence were collected using 450±50 and 575±25-nm band-pass filters. Gating and scoring were done with Flowjo program. G_2/M cells were identified by double DNA content. The RNA threshold was set at the lowest RNA content of G_2/M cells. Cells with RNA content below the threshold are categorized as G_0.

Immunofluorescence

Cells were plated at ~5% confluence in chamber slides, and then starved in DMEM with 0.5% FBS for 48 hr. Cells were fixed with 100 µl 3% paraformaldehyde in PBS for 20 min at room temperature, and then washed 2 times with 500 µl PBS for 5 min, and permeabilized with 1% goat serum and 0.5% Triton-X100 in PBS for 15 min at room temperature. After 3 washes with 500 µl 1% goat serum in PBS, cells were incubated with 100 µl diluted anti-Ki67 (Abcam; 1:50) in PBS and 1% goat serum for 1 hr. After 2 washes with 500 µl 1% goat serum in PBS, cells were incubated with Alexa-488 conjugated anti-rabbit IgG (H+L) (Invitrogen, 1:1000) diluted in 100 µl PBS with 1% goat serum. Cells were then stained with 1µg.ml DAPI in 100 µl PBS with 1% goat serum. After washing with 500 µl H_2O, top of chamber slide and remaining liquid are removed. Cells are air-dried and mounted with coverslip, sealed with nail polish. Images were taken under the 40x objective, with immersion oil. Images were processed with CellProfiler, counting cells and scoring the percentage of cells stained with Ki-67,

with setting adapted from the ExamplePercentPositive pipeline available on the program website.

3.6 Acknowledgements

Chapter 3, in part, is currently being prepared for submission for publication of the material as Fu R., Lykke-Andersen J. The dissertation author was the primary investigator and author of this material.

Chapter 4. Conclusions and future directions

4.1 Conclusions

Although controlled mRNA decay has gained increasing recognition for its importance in gene expression regulation, many finer details of its mechanisms and regulations remain unclear.

Concerning molecular mechanisms, co-factors of AMD, besides the degradation enzymes, have not been documented extensively. Previous work from the lab on exogenously expressed flag-TTP in 293T cells revealed a novel interaction with hnRNP F, which stimulated the decay on a subset of TTP targets (68). In Chapter 2, I described TTP associating with a translation repressing complex 4EHP-GYF2 during LPS-induced macrophage innate immune response. This interaction was not observed from previous TTP or 4EHP co-IP mass spectrometry analyses from HeLa and 293T cells, suggesting co-factor availability may differ greatly between cell types, and that choosing physiologically relevant systems for query is crucial. Through co-immunoprecipitation and in vitro pull down experiments, we demonstrated that GYF2 interacts directly with PPPPGF motifs of mouse TTP, and 4EHP is recruited indirectly. It is noteworthy that mutation of all tetraproline motifs of TTP did not completely abolish 4EHP-GYF2 association to TTP, whereas deletion of the RBD and CTD did. It is possible that 4EHP or GYF2 also weakly interacts with other regions of TTP, or other TTP co-factors. In any case, the NTD was necessary for 4EHP-GYF2-TTP co-purification, and among the three tetraprolines the NTD PPPPGF motif also led to the strongest loss of interaction when mutated. Functionally, I observed a deficiency in gene repression, most likely translational repression, by the tetraproline mutant in luciferase reporter assays. Further work in 4EHP knockout MEFs also showed 4EHP involvement in TTP-mediated decay of previously established targets. I conclude

4EHP-GYF2 are co-factors of TTP function. Notably, 4EHP-GYF2 association with TTP is not impacted by CIM deletion, and likewise CNOT-1 binding to TTP is undisturbed in the tetraproline mutants. This suggests TTP recruits 4EHP-GYF2 and CCR4-NOT independently of each other.

Our attempts at testing 4EHP-GYF2-TTP translation repression activity *in vitro* yielded results difficult to interpret. *In vitro* translation assays with rabbit reticulocyte lysate and capped ARE-containing reporter mRNA showed ~20% translation repression when 4EHP, GYF2 and TTP were added into the reaction. Optimization of protein/RNA ratio, incubation time length, and zinc concentration did not enhance repression. One possible explanation is that our experiment does not include any other cellular factors also facilitating the translation repression process. Alternatively, protein impurity, incorrect re-folding, or degradation of our purified proteins may have obscured the effect.

Functionally, the contribution of AMD to cellular processes outside of the immune response remains poorly understood. TTP and its homologs BRF1 and BRF2, in particular, are highly inducible by many stimuli, and may therefore be involved in rapid gene expression control in those systems. In Chapter 3, I examined the effects of TTP and homologs on G0-G1-S cell cycle transition. TTP and BRF1 are highly induced during the initial hours of serum activation after starvation, whereas BRF2 rose in mRNA and protein levels as TTP and BRF1 decreased. I describe a modest slowdown of cell cycle transition in NIH/3T3 cells treated with siRNAs against the TTP family. In TTP family protein-depleted cells, E2F target transcription was repressed, and Rb family mRNAs were stabilized. This was consistent with previous reports of overexpression or knockdown of HuR, a TTP-antagonizing AUBP, impacting the cell cycle modestly. Since several other factors in the CDK-RB-E2F pathway also contain

AREs, it is possible AMD may facilitate transition or stalling of the replication cycle depending on the mRNA levels of potential targets, the availability of different co-factors, and cell signaling. In support of this dynamic view, recent reports point to BRF1 and BRF2 playing opposite role in self-renewal of different pluripotent cell types (32, 33).

Of course, my work only raises more questions for future investigation.

4.2 How does translation repression by 4EHP-GYF2 affect mRNA decay?

The 4EHP-GYF2 complex has a documented repressing effect on translation initiation, but I found evidence that mRNA decay activated by TTP was also affected by 4EHP. 4EHP knockout mouse embryonic fibroblasts accumulate TTP target mRNAs to much higher level compared to wild-type cells during serum activation. Furthermore, mRNA turnover of those mRNA were indeed slowed compared to wild-type cells, from Actinomycin D decay assays. At present we do not have clear data on how this impact on decay is achieved by 4EHP and/or GYF2. One hypothesis is that 4EHP-GYF2 recruitment by TTP orients and/or locally enriches the complex to compete with eIF4E for the 5' cap, and displacing eIF4F from the mRNP. Aside from potential easier access to the cap for decapping machinery, this change has greater implications on mRNP architecture. Without eIF4G interacting with PABP, the poly(A)-tail may no longer be associating near the cap in the canonical loop structure, possibly rendering it more vulnerable for deadenylation.

Another alternative, though not exclusive, model would involve other proteins being recruited by 4EHP and/or GYF2 to the TTP-bound mRNA. GYF2 in particular is a large protein, around 180kD with relatively few identified domains/motifs, making it

an attractive candidate for co-factor association. IP and mass spectrometry analysis of associating factors to the protein may shed more light on its functions.

The first step towards understanding the role of 4EHP-GYF2 in decay would be to assess whether cap-binding deficient mutant of 4EHP can rescue the impaired decay I observed in 4EHP knockout MEFs. Another direction is to pinpoint which exact step(s) of the decay process are stalled when 4EHP is limited. With northern blot detection of cytokine and reporter mRNAs, I did not observe a characteristic pattern for deadenylated mRNA decay intermediates. This suggests deadenylation, which occurs before decapping, may be affected, or that the deficiency was not prominent enough for visualization by northern blotting. Notably, the tetraproline mutant of TTP, with little binding to 4EHP and GYF2, associated with similar amounts of RNA in an RNA-IP experiment, suggesting that 4EHP-GYF2 does not guide TTP binding to RNA (Figure 2.15).

4.3 How is 4EHP-GYF2-TTP repression activity regulated?

After concluding the 4EHP-GYF2 is recruited by TTP via the tetraproline motifs, we wondered whether this co-factor is constitutively associated with TTP, or only binding to a subset of TTP molecules in the suitable context. Co-IP experiments with other established TTP mutants exclude some possibilities. The RNA-binding mutant F118N (adapted from human mutant previously described, (106)) co-purified with 4EHP and GYF2 (data not show). So did the S52A S178A mutant, which has key MK2 phosphorylation sites mutated and does not lose CNOT-binding ability upon hyperphosphorylation (Figure 2.16). Together with the domain truncation results, it appears 4EHP-GYF2-TTP complex formation is not affected by RNA-binding and CNOT-binding status of TTP. Additionally, CNOT1 (deadenylase subunit), Dcp1a

(decapping subunit) and Xrn1 (5'-3' exonuclease) all co-purify with tetraproline mutant of TTP (Figure 2.16), suggesting impaired recruitment of 4EHP and GYF2 does not interfere with assembly of known decay machinery. Dcp1a, Xrn1 and an exosome subunit Rrp45 also associated with exogenously expressed 4EHP and GYF2, suggesting recruitment of decay machinery and the translational repression complex is not exclusive (Figure 2.17). The caveat of these interpretations, is of course that overexpression of proteins may disrupt the usual balance of protein interactions.

Also of interest is whether the phosphorylation state of TTP affects 4EHP-GYF2 binding. Only p38-MK2 phosphorylation has been pinpointed to affect TTP function, but I have evidence that 4EHP-GYF2 is not affected in the same way CCR4-NOT is to phosphorylation. It is therefore tempting to speculate that 4EHP-GYF2-TTP interaction remains intact and may serve to repress translation and/or influence decay when other co-factor complexes of TTP are restricted. Whether any specific phosphorylation modifications impact TTP-mediated repression by 4EHP-GYF2 will require further investigations. Interestingly, in TTP knockout MEFs, a smaller portion of the TTP tetraproline mutant appears to be slow-migrating on SDS PAGE, compared to exogenous wild-type TTP (Figure 2.9B). Since the higher molecular weight band collapses with phosphatase treatment, it does hint at abnormal phosphorylation of the mutant.

Another intriguing possibility is that 4EHP or GYF2 could be regulated via cell signaling, to disrupt or facilitate the TTP-mediated mRNP complex. 4EHP is post-translationally modified by ISG15 during interferon induced immune responses, which increases its affinity to the methylated cap (107). This potentially leads to stronger ability to displace the eIF4F complex, and stronger translational repression and/or mRNA decay. GYF2 was first described as a Grb10-interacting protein, also via a

tetraproline motif on Grb10. Grb10 is an adaptor protein to a group of receptor tyrosine kinases. Therefore we could imagine a scenario where insulin and insulin-like growth factor signaling would tip the balance toward Grb10 in its competition with TTP for GYF2 recruitment.

4.4 What other features distinguish the TTP family homologs?

A fascinating question fueling my research in the beginning was how did the TTP family homologs differ in function or target specificity. Although recent publications provided high-throughput datasets of TTP, BRF1 and BRF2 RNA-IP, none are performed from the same cell lines, and no further efforts to determine additional sequence or secondary structure preference has been carried out, to my knowledge. In my work, with the limited number of mRNAs tested in TTP and BRF1 immunoprecipitations, no distinctions stand out. In decay assays with single siRNA toward one of the homologs, stabilization was only observed in some AUBP-RNA-time combinations. However, it is difficult to discern whether these differences stem from expression timing of the zinc finger proteins, siRNA knockdown efficiency, or actual target preference. Unfortunately I did not have the time to further pursue the question.

I did inadvertently stumble upon a difference in co-factor recruitment among the three homologs. Of the family, only TTP contains conserved PPPPGF motifs, and co-IP experiments confirmed 4EHP-GYF2 are not strongly enriched in BRF1 or BRF2 IPs. TTP, BRF1 and BRF2 share similar RNA-binding motifs and CNOT1-interacting motifs. Previous efforts from the lab also identified that both TTP and BRF1 (BRF2 was not included in the experiment) associate with hnRNP F. Therefore 4EHP-GYF2 recruitment is a rare example of one protein in the family behaving in a unique manner. Considering the homology between BRF1 and BRF2 is much higher than that between

TTP and either homolog, other distinct features might exist. For example, an idea that I briefly considered pursuing, BRF1 and BRF2 contain ATM and DNA-PK phosphorylation sites conserved from fish to mammals, but TTP does not. I did confirm induction and hyperphosphorylation of BRF1 during the DNA damage response induced by doxorubicin, which is known to activate ATM and DNA-PK. Based on previous knowledge of TTP modifications, phosphorylation may stabilize the protein, alter subcellular localization, and/or affect decay activity.

4.5 How do other *cis* and trans elements affect TTP-mediated activity?

Within the 7% of genes predicted to harbor AUUUA core pentamers in their mRNA 3'UTR, some are clearly impacted more than others by abnormal AMD. Several algorithms have been developed, highlighting the number of ARE repeats and their distance in determining AUBP recognition of the *cis* element. Alternatively, since multiple *cis* elements triggering different pathways may sit on the same mRNA molecule, higher affinity or efficiency pathways may mask the others. For instance, c-fos in past chapters was used as a negative control not affected by TTP overexpression or knockdown. It in fact contains a well-established ARE, but in cell culture conditions TTP is not rate-limiting for its decay, due to additional instability elements (108). It is also likely that binding of one *cis*-trans element pair can inhibit or facilitate proper binding of another pair. A couple of studies report TTP and AUF1 associating with RISC to target a few mRNAs (109, 110), but the interaction is not commonly seen (for instance, not in our IP-LC-MS/MS assays). Although the RNA-binding landscape of individual proteins have been mapped through cross-linking based sequencing techniques, we still understand very little of how various RNA-binding proteins associate on the same RNA molecule.

References

1. Komili S Silver PA (2008) Coupling and coordination in gene expression processes: a systems biology view. *Nat Rev Genet* 9(1):38-48.

2. Glisovic T, Bachorik JL, Yong J, Dreyfuss G (2008) RNA-binding proteins and post-transcriptional gene regulation. *FEBS Lett* 582(14):1977-1986.

3. Rabani M, Levin JZ, Fan L, Adiconis X, Raychowdhury R, Garber M, Gnirke A, Nusbaum C, Hacohen N, Friedman N, Amit I, Regev A (2011) Metabolic labeling of RNA uncovers principles of RNA production and degradation dynamics in mammalian cells. *Nat Biotechnol* 29(5):436-442.

4. Hao S Baltimore D (2009) The stability of mRNA influences the temporal order of the induction of genes encoding inflammatory molecules. *Nat Immunol* 10(3):281-288.

5. Reznik B Lykke-Andersen J (2010) Regulated and quality-control mRNA turnover pathways in eukaryotes. *Biochem Soc Trans* 38(6):1506-1510.

6. Garneau NL, Wilusz J, Wilusz CJ (2007) The highways and byways of mRNA decay. *Nat Rev Mol Cell Biol* 8(2):113-126.

7. Gebauer F, Preiss T, Hentze MW (2012) From cis-regulatory elements to complex RNPs and back. *Cold Spring Harb Perspect Biol* 4(7):a012245.

8. Gruber AR, Fallmann J, Kratochvill F, Kovarik P, Hofacker IL (2011) AREsite: a database for the comprehensive investigation of AU-rich elements. *Nucleic Acids Res* 39(Database issue):D66-69.

9. Wang W, Fan J, Yang X, Furer-Galban S, Lopez de Silanes I, von Kobbe C, Guo J, Georas SN, Foufelle F, Hardie DG, Carling D, Gorospe M (2002) AMP-activated kinase regulates cytoplasmic HuR. *Mol Cell Biol* 22(10):3425-3436.

10. Raineri I, Wegmueller D, Gross B, Certa U, Moroni C (2004) Roles of AUF1 isoforms, HuR and BRF1 in ARE-dependent mRNA turnover studied by RNA interference. *Nucleic Acids Research* 32(4):1279-1288.

11. Brooks SA Blackshear PJ (2013) Tristetraprolin (TTP): interactions with mRNA and proteins, and current thoughts on mechanisms of action. *Biochim Biophys Acta* 1829(6-7):666-679.

12. Hudson BP, Martinez-Yamout MA, Dyson HJ, Wright PE (2004) Recognition of the mRNA AU-rich element by the zinc finger domain of TIS11d. *Nat Struct Mol Biol* 11(3):257-264.

13. Lykke-Andersen J Wagner E (2005) Recruitment and activation of mRNA decay enzymes by two ARE-mediated decay activation domains in the proteins TTP and BRF-1. *Genes Dev* 19(3):351-361.

14. Fabian MR, Frank F, Rouya C, Siddiqui N, Lai WS, Karetnikov A, Blackshear PJ, Nagar B, Sonenberg N (2013) Structural basis for the recruitment of the human CCR4-NOT deadenylase complex by tristetraprolin. *Nat Struct Mol Biol* 20(6):735-739.

15. Taylor GA, Carballo E, Lee DM, Lai WS, Thompson MJ, Patel DD, Schenkman DI, Gilkeson GS, Broxmeyer HE, Haynes BF, Blackshear PJ (1996) A pathogenetic role for TNF alpha in the syndrome of cachexia, arthritis, and autoimmunity resulting from tristetraprolin (TTP) deficiency. *Immunity* 4(5):445-454.

16. Lai WS, Parker JS, Grissom SF, Stumpo DJ, Blackshear PJ (2006) Novel mRNA targets for tristetraprolin (TTP) identified by global analysis of stabilized transcripts in TTP-deficient fibroblasts. *Mol Cell Biol* 26(24):9196-9208.

17. Stoecklin G, Tenenbaum SA, Mayo T, Chittur SV, George AD, Baroni TE, Blackshear PJ, Anderson P (2008) Genome-wide analysis identifies interleukin-10 mRNA as target of tristetraprolin. *Journal of Biological Chemistry* 283(17):11689-11699.

18. Al-Souhibani N, Al-Ahmadi W, Hesketh JE, Blackshear PJ, Khabar KS (2010) The RNA-binding zinc-finger protein tristetraprolin regulates AU-rich mRNAs involved in breast cancer-related processes. *Oncogene* 29(29):4205-4215.

19. Brook M, Tchen CR, Santalucia T, McIlrath J, Arthur JS, Saklatvala J, Clark AR (2006) Posttranslational regulation of tristetraprolin subcellular localization and protein stability by p38 mitogen-activated protein kinase and extracellular signal-regulated kinase pathways. *Mol Cell Biol* 26(6):2408-2418.

20. Mahtani KR, Brook M, Dean JL, Sully G, Saklatvala J, Clark AR (2001) Mitogen-activated protein kinase p38 controls the expression and posttranslational modification of tristetraprolin, a regulator of tumor necrosis factor alpha mRNA stability. *Mol Cell Biol* 21(19):6461-6469.

21. Cao HP, Deterding LJ, Venable JD, Kennington EA, Yates JR, Tomer KB, Blackshear PJ (2006) Identification of the anti-inflammatory protein tristetraprolin as a hyperphosphorylated protein by mass spectrometry and site-directed mutagenesis. *Biochemical Journal* 394:285-297.

22. Chrestensen CA, Schroeder MJ, Shabanowitz J, Hunt DF, Pelo JW, Worthington MT, Sturgill TW (2004) MAPKAP kinase 2 phosphorylates tristetraprolin on in vivo sites including Ser178, a site required for 14-3-3 binding. *J Biol Chem* 279(11):10176-10184.

23. Stoecklin G, Stubbs T, Kedersha N, Wax S, Rigby WF, Blackwell TK, Anderson P (2004) MK2-induced tristetraprolin:14-3-3 complexes prevent stress granule association and ARE-mRNA decay. *EMBO J* 23(6):1313-1324.

24. Clement SL, Scheckel C, Stoecklin G, Lykke-Andersen J (2011) Phosphorylation of Tristetraprolin by MK2 Impairs AU-Rich Element mRNA

Decay by Preventing Deadenylase Recruitment. *Molecular and Cellular Biology* 31(2):256-266.

25. Sun L, Stoecklin G, Van Way S, Hinkovska-Galcheva V, Guo RF, Anderson P, Shanley TP (2007) Tristetraprolin (TTP)-14-3-3 complex formation protects TTP from dephosphorylation by protein phosphatase 2a and stabilizes tumor necrosis factor-alpha mRNA. *J Biol Chem* 282(6):3766-3777.

26. Schichl YM, Resch U, Lemberger CE, Stichlberger D, de Martin R (2011) Novel phosphorylation-dependent ubiquitination of tristetraprolin by mitogen-activated protein kinase/extracellular signal-regulated kinase kinase kinase 1 (MEKK1) and tumor necrosis factor receptor-associated factor 2 (TRAF2). *J Biol Chem* 286(44):38466-38477.

27. Qi MY, Wang ZZ, Zhang Z, Shao Q, Zeng A, Li XQ, Li WQ, Wang C, Tian FJ, Li Q, Zou J, Qin YW, Brewer G, Huang S, Jing Q (2012) AU-rich-element-dependent translation repression requires the cooperation of tristetraprolin and RCK/P54. *Mol Cell Biol* 32(5):913-928.

28. Schott J, Reitter S, Philipp J, Haneke K, Schafer H, Stoecklin G (2014) Translational regulation of specific mRNAs controls feedback inhibition and survival during macrophage activation. *PLoS Genet* 10(6):e1004368.

29. Blackshear PJ, Phillips RS, Ghosh S, Ramos SB, Richfield EK, Lai WS (2005) Zfp36l3, a rodent X chromosome gene encoding a placenta-specific member of the Tristetraprolin family of CCCH tandem zinc finger proteins. *Biol Reprod* 73(2):297-307.

30. Stumpo DJ, Byrd NA, Phillips RS, Ghosh S, Maronpot RR, Castranio T, Meyers EN, Mishina Y, Blackshear PJ (2004) Chorioallantoic fusion defects and embryonic lethality resulting from disruption of Zfp36L1, a gene encoding a CCCH tandem zinc finger protein of the Tristetraprolin family. *Mol Cell Biol* 24(14):6445-6455.

31. Stumpo DJ, Broxmeyer HE, Ward T, Cooper S, Hangoc G, Chung YJ, Shelley WC, Richfield EK, Ray MK, Yoder MC, Aplan PD, Blackshear PJ (2009) Targeted disruption of Zfp36l2, encoding a CCCH tandem zinc finger RNA-binding protein, results in defective hematopoiesis. *Blood* 114(12):2401-2410.

32. Zhang LB, Prak L, Rayon-Estrada V, Thiru P, Flygare J, Lim B, Lodish HF (2013) ZFP36L2 is required for self-renewal of early burst-forming unit erythroid progenitors. *Nature* 499(7456):92-+.

33. Tan FE Elowitz MB (2014) Brf1 posttranscriptionally regulates pluripotency and differentiation responses downstream of Erk MAP kinase. *Proc Natl Acad Sci U S A* 111(17):E1740-1748.

34. Lu JY Schneider RJ (2004) Tissue distribution of AU-rich mRNA-binding proteins involved in regulation of mRNA decay. *J Biol Chem* 279(13):12974-12979.

35. Kim MS, Pinto SM, Getnet D, Nirujogi RS, Manda SS, Chaerkady R, Madugundu AK, Kelkar DS, Isserlin R, Jain S, Thomas JK, Muthusamy B, Leal-Rojas P, Kumar P, Sahasrabuddhe NA, Balakrishnan L, Advani J, George B, Renuse S, Selvan LD, Patil AH, Nanjappa V, Radhakrishnan A, Prasad S, Subbannayya T, Raju R, Kumar M, Sreenivasamurthy SK, Marimuthu A, Sathe GJ, Chavan S, Datta KK, Subbannayya Y, Sahu A, Yelamanchi SD, Jayaram S, Rajagopalan P, Sharma J, Murthy KR, Syed N, Goel R, Khan AA, Ahmad S, Dey G, Mudgal K, Chatterjee A, Huang TC, Zhong J, Wu X, Shaw PG, Freed D, Zahari MS, Mukherjee KK, Shankar S, Mahadevan A, Lam H, Mitchell CJ, Shankar SK, Satishchandra P, Schroeder JT, Sirdeshmukh R, Maitra A, Leach SD, Drake CG, Halushka MK, Prasad TS, Hruban RH, Kerr CL, Bader GD, Iacobuzio-Donahue CA, Gowda H, Pandey A (2014) A draft map of the human proteome. *Nature* 509(7502):575-581.

36. Hodson DJ, Janas ML, Galloway A, Bell SE, Andrews S, Li CM, Pannell R, Siebel CW, MacDonald HR, De Keersmaecker K, Ferrando AA, Grutz G, Turner M (2010) Deletion of the RNA-binding proteins ZFP36L1 and ZFP36L2 leads to perturbed thymic development and T lymphoblastic leukemia. *Nat Immunol* 11(8):717-724.

37. Ball CB, Rodriguez KF, Stumpo DJ, Ribeiro-Neto F, Korach KS, Blackshear PJ, Birnbaumer L, Ramos SB (2014) The RNA-binding protein, ZFP36L2, influences ovulation and oocyte maturation. *PLoS One* 9(5):e97324.

38. Benjamin D, Schmidlin M, Min L, Gross B, Moroni C (2006) BRF1 protein turnover and mRNA decay activity are regulated by protein kinase B at the same phosphorylation sites. *Molecular and Cellular Biology* 26(24):9497-9507.

39. Ramos SB (2012) Characterization of DeltaN-Zfp36l2 mutant associated with arrest of early embryonic development and female infertility. *J Biol Chem* 287(16):13116-13127.

40. Lai WS, Stumpo DJ, Kennington EA, Burkholder AB, Ward JM, Fargo DL, Blackshear PJ (2013) Life without TTP: apparent absence of an important anti-inflammatory protein in birds. *Am J Physiol-Reg I* 305(7):R689-R700.

41. von der Haar T, Gross JD, Wagner G, McCarthy JE (2004) The mRNA cap-binding protein eIF4E in post-transcriptional gene expression. *Nat Struct Mol Biol* 11(6):503-511.

42. Goss DJ Kleiman FE (2013) Poly(A) binding proteins: are they all created equal? *Wires Rna* 4(2):167-179.

43. Pillai RS, Artus CG, Filipowicz W (2004) Tethering of human Ago proteins to mRNA mimics the miRNA-mediated repression of protein synthesis. *RNA* 10(10):1518-1525.

44. Pfeiffer JR Brooks SA (2012) Cullin 4B is recruited to tristetraprolin-containing messenger ribonucleoproteins and regulates TNF-alpha mRNA polysome loading. *J Immunol* 188(4):1828-1839.

45. Wharton RP, Sonoda J, Lee T, Patterson M, Murata Y (1998) The Pumilio RNA-binding domain is also a translational regulator. *Molecular Cell* 1(6):863-872.

46. Pause A, Belsham GJ, Gingras AC, Donze O, Lin TA, Lawrence JC, Sonenberg N (1994) Insulin-Dependent Stimulation of Protein-Synthesis by Phosphorylation of a Regulator of 5'-Cap Function. *Nature* 371(6500):762-767.

47. Marcotrigiano J, Gingras AC, Sonenberg N, Burley SK (1999) Cap-dependent translation initiation in eukaryotes is regulated by a molecular mimic of eIF4G. *Molecular Cell* 3(6):707-716.

48. Dostie J, Ferraiuolo M, Pause A, Adam SA, Sonenberg N (2000) A novel shuttling protein, 4E-T, mediates the nuclear import of the mRNA 5 ' cap-binding protein, eIF4E. *Embo Journal* 19(12):3142-3156.

49. Rajyaguru P, She MP, Parker R (2012) Scd6 Targets eIF4G to Repress Translation: RGG Motif Proteins as a Class of eIF4G-Binding Proteins. *Molecular Cell* 45(2):244-254.

50. Rom E, Kim HC, Gingras AC, Marcotrigiano J, Favre D, Olsen H, Burley SK, Sonenberg N (1998) Cloning and characterization of 4EHP, a novel mammalian eIF4E-related cap-binding protein. *J Biol Chem* 273(21):13104-13109.

51. Joshi B, Cameron A, Jagus R (2004) Characterization of mammalian eIF4E-family members. *Eur J Biochem* 271(11):2189-2203.

52. Cho PF, Poulin F, Cho-Park YA, Cho-Park IB, Chicoine JD, Lasko P, Sonenberg N (2005) A new paradigm for translational control: inhibition via 5'-3' mRNA tethering by Bicoid and the eIF4E cognate 4EHP. *Cell* 121(3):411-423.

53. Morita M, Ler LW, Fabian MR, Siddiqui N, Mullin M, Henderson VC, Alain T, Fonseca BD, Karashchuk G, Bennett CF, Kabuta T, Higashi S, Larsson O, Topisirovic I, Smith RJ, Gingras AC, Sonenberg N (2012) A novel 4EHP-GIGYF2 translational repressor complex is essential for mammalian development. *Mol Cell Biol* 32(17):3585-3593.

54. Carballo E, Lai WS, Blackshear PJ (1998) Feedback inhibition of macrophage tumor necrosis factor-alpha production by tristetraprolin. *Science* 281(5379):1001-1005.

55. Carballo E, Lai WS, Blackshear PJ (2000) Evidence that tristetraprolin is a physiological regulator of granulocyte-macrophage colony-stimulating factor messenger RNA deadenylation and stability. *Blood* 95(6):1891-1899.

56. Fenger-Gron M, Fillman C, Norrild B, Lykke-Andersen J (2005) Multiple processing body factors and the ARE binding protein TTP activate mRNA decapping. *Molecular Cell* 20(6):905-915.

57. Sandler H, Kreth J, Timmers HT, Stoecklin G (2011) Not1 mediates recruitment of the deadenylase Caf1 to mRNAs targeted for degradation by tristetraprolin. *Nucleic Acids Res* 39(10):4373-4386.

58. Lai WS, Kennington EA, Blackshear PJ (2003) Tristetraprolin and its family members can promote the cell-free deadenylation of AU-rich element-containing mRNAs by poly(A) ribonuclease. *Molecular and Cellular Biology* 23(11):3798-3812.

59. Lehner B Sanderson CM (2004) A protein interaction framework for human mRNA degradation. *Genome Res* 14(7):1315-1323.

60. Chen CY, Gherzi R, Ong SE, Chan EL, Raijmakers R, Pruijn GJ, Stoecklin G, Moroni C, Mann M, Karin M (2001) AU binding proteins recruit the exosome to degrade ARE-containing mRNAs. *Cell* 107(4):451-464.

61. Hitti E, Iakovleva T, Brook M, Deppenmeier S, Gruber AD, Radzioch D, Clark AR, Blackshear PJ, Kotlyarov A, Gaestel M (2006) Mitogen-activated protein kinase-activated protein kinase 2 regulates tumor necrosis factor mRNA stability and translation mainly by altering tristetraprolin expression, stability, and binding to adenine/uridine-rich element. *Molecular and Cellular Biology* 26(6):2399-2407.

62. Lai WS, Stumpo DJ, Blackshear PJ (1990) Rapid insulin-stimulated accumulation of an mRNA encoding a proline-rich protein. *J Biol Chem* 265(27):16556-16563.

63. Ciais D, Cherradi N, Bailly S, Grenier E, Berra E, Pouyssegur J, Lamarre J, Feige JJ (2004) Destabilization of vascular endothelial growth factor mRNA by the zinc-finger protein TIS11b. *Oncogene* 23(53):8673-8680.

64. Hodson DJ, Janas ML, Galloway A, Bell SE, Andrews S, Li CM, Pannell R, Siebel CW, MacDonald HR, De Keersmaecker K, Ferrando AA, Grutz G, Turner M (2010) Deletion of the RNA-binding proteins ZFP36L1 and ZFP36L2 leads to perturbed thymic development and T lymphoblastic leukemia (vol 11, pg 717, 2010). *Nat Immunol* 11(10):969-969.

65. Tao X Gao G (2015) Tristetraprolin recruits eIF4E2 to repress translation of ARE-containing mRNAs. *Mol Cell Biol*.

66. Lau NC, Kolkman A, van Schaik FM, Mulder KW, Pijnappel WW, Heck AJ, Timmers HT (2009) Human Ccr4-Not complexes contain variable deadenylase subunits. *Biochem J* 422(3):443-453.

67. Johnson BA, Stehn JR, Yaffe MB, Blackwell TK (2002) Cytoplasmic localization of tristetraprolin involves 14-3-3-dependent and -independent mechanisms. *J Biol Chem* 277(20):18029-18036.

68. Reznik B, Clement SL, Lykke-Andersen J (2014) hnRNP F complexes with tristetraprolin and stimulates ARE-mRNA decay. *PLoS One* 9(6):e100992.

69. Freund C, Dotsch V, Nishizawa K, Reinherz EL, Wagner G (1999) The GYF domain is a novel structural fold that is involved in lymphoid signaling through proline-rich sequences. *Nat Struct Biol* 6(7):656-660.

70. Kofler M, Motzny K, Freund C (2005) GYF domain proteomics reveals interaction sites in known and novel target proteins. *Mol Cell Proteomics* 4(11):1797-1811.

71. Stoecklin G, Stoeckle P, Lu M, Muehlemann O, Moroni C (2001) Cellular mutants define a common mRNA degradation pathway targeting cytokine AU-rich elements. *Rna-a Publication of the Rna Society* 7(11):1578-1588.

72. Johnson BA Blackwell TK (2002) Multiple tristetraprolin sequence domains required to induce apoptosis and modulate responses to TNF alpha through distinct pathways. *Oncogene* 21(27):4237-4246.

73. Ohnishi T, Yamashita A, Kashima I, Schell T, Anders KR, Grimson A, Hachiya T, Hentze MW, Anderson P, Ohno S (2003) Phosphorylation of hUPF1 induces formation of mRNA surveillance complexes containing hSMG-5 and hSMG-7. *Mol Cell* 12(5):1187-1200.

74. Fukuhara N, Ebert J, Unterholzner L, Lindner D, Izaurralde E, Conti E (2005) SMG7 is a 14-3-3-like adaptor in the nonsense-mediated mRNA decay pathway. *Molecular Cell* 17(4):537-547.

75. Eberle AB, Lykke-Andersen S, Muhlemann O, Jensen TH (2009) SMG6 promotes endonucleolytic cleavage of nonsense mRNA in human cells. *Nat Struct Mol Biol* 16(1):49-55.

76. Huntzinger E Izaurralde E (2011) Gene silencing by microRNAs: contributions of translational repression and mRNA decay. *Nat Rev Genet* 12(2):99-110.

77. Goldstrohm AC, Hook BA, Seay DJ, Wickens M (2006) PUF proteins bind Pop2p to regulate messenger RNAs. *Nature Structural & Molecular Biology* 13(6):533-539.

78. Weidmann CA Goldstrohm AC (2012) Drosophila Pumilio Protein Contains Multiple Autonomous Repression Domains That Regulate mRNAs Independently of Nanos and Brain Tumor. *Molecular and Cellular Biology* 32(2):527-540.

79. Lykke-Andersen J (2002) Identification of a human decapping complex associated with hUpf proteins in nonsense-mediated decay. *Mol Cell Biol* 22(23):8114-8121.

80. Lykke-Andersen J, Shu MD, Steitz JA (2000) Human Upf proteins target an mRNA for nonsense-mediated decay when bound downstream of a termination codon. *Cell* 103(7):1121-1131.

81. Voeltz GK Steitz JA (1998) AUUUA sequences direct mRNA deadenylation uncoupled from decay during Xenopus early development. *Mol Cell Biol* 18(12):7537-7545.

82. Erickson SL, Corpuz EO, Maloy JP, Fillman C, Webb K, Bennett EJ, Lykke-Andersen J (2015) Competition between Decapping Complex Formation and Ubiquitin-Mediated Proteasomal Degradation Controls Human Dcp2 Decapping Activity. *Mol Cell Biol* 35(12):2144-2153.

83. Nielsen J, Christiansen J, Lykke-Andersen J, Johnsen AH, Wewer UM, Nielsen FC (1999) A family of insulin-like growth factor II mRNA-binding proteins represses translation in late development. *Mol Cell Biol* 19(2):1262-1270.

84. Nurse P (2000) A long twentieth century of the cell cycle and beyond. *Cell* 100(1):71-78.

85. Bertoli C, Skotheim JM, de Bruin RA (2013) Control of cell cycle transcription during G1 and S phases. *Nat Rev Mol Cell Biol* 14(8):518-528.

86. Harbour JW Dean DC (2000) The Rb/E2F pathway: expanding roles and emerging paradigms. *Genes Dev* 14(19):2393-2409.

87. Weinberg RA (1995) The retinoblastoma protein and cell cycle control. *Cell* 81(3):323-330.

88. Chellappan SP, Hiebert S, Mudryj M, Horowitz JM, Nevins JR (1991) The E2f Transcription Factor Is a Cellular Target for the Rb Protein. *Cell* 65(6):1053-1061.

89. Cao L, Faha B, Dembski M, Tsai LH, Harlow E, Dyson N (1992) Independent binding of the retinoblastoma protein and p107 to the transcription factor E2F. *Nature* 355(6356):176-179.

90. Cobrinik D, Whyte P, Peeper DS, Jacks T, Weinberg RA (1993) Cell Cycle-Specific Association of E2f with the P130 E1a-Binding Protein. *Gene Dev* 7(12A):2392-2404.

91. Weintraub SJ, Prater CA, Dean DC (1992) Retinoblastoma protein switches the E2F site from positive to negative element. *Nature* 358(6383):259-261.

92. Mittnacht S (1998) Control of pRB phosphorylation. *Curr Opin Genet Dev* 8(1):21-27.

93. Chittenden T, Livingston DM, DeCaprio JA (1993) Cell cycle analysis of E2F in primary human T cells reveals novel E2F complexes and biochemically distinct forms of free E2F. *Mol Cell Biol* 13(7):3975-3983.

94. Leone G, DeGregori J, Yan Z, Jakoi L, Ishida S, Williams RS, Nevins JR (1998) E2F3 activity is regulated during the cell cycle and is required for the induction of S phase. *Gene Dev* 12(14):2120-2130.

95. Smith EJ, Leone G, DeGregori J, Jakoi L, Nevins JR (1996) The accumulation of an E2F-p130 transcriptional repressor distinguishes a G0 cell state from a G1 cell state. *Mol Cell Biol* 16(12):6965-6976.

96. Raghavan A, Ogilvie RL, Reilly C, Abelson ML, Raghavan S, Vasdewani J, Krathwohl M, Bohjanen PR (2002) Genome-wide analysis of mRNA decay in resting and activated primary human T lymphocytes. *Nucleic Acids Res* 30(24):5529-5538.

97. Spasic M, Friedel CC, Schott J, Kreth J, Leppek K, Hofmann S, Ozgur S, Stoecklin G (2012) Genome-wide assessment of AU-rich elements by the AREScore algorithm. *PLoS Genet* 8(1):e1002433.

98. Lebedeva S, Jens M, Theil K, Schwanhausser B, Selbach M, Landthaler M, Rajewsky N (2011) Transcriptome-wide Analysis of Regulatory Interactions of the RNA-Binding Protein HuR. *Molecular Cell* 43(3):340-352.

99. Al-Ahmadi W, Al-Ghamdi M, Al-Souhibani N, Khabar KS (2013) miR-29a inhibition normalizes HuR over-expression and aberrant AU-rich mRNA stability in invasive cancer. *J Pathol* 230(1):28-38.

100. Vaites LP, Lee EK, Lian Z, Barbash O, Roy D, Wasik M, Klein-Szanto AJ, Rustgi AK, Diehl JA (2011) The Fbx4 tumor suppressor regulates cyclin D1 accumulation and prevents neoplastic transformation. *Mol Cell Biol* 31(22):4513-4523.

101. Darzynkiewicz Z, Evenson DP, Staianocoico L, Sharpless TK, Melamed ML (1979) Correlation between Cell-Cycle Duration and Rna-Content. *Journal of Cellular Physiology* 100(3):425-438.

102. Gerdes J, Schwab U, Lemke H, Stein H (1983) Production of a mouse monoclonal antibody reactive with a human nuclear antigen associated with cell proliferation. *Int J Cancer* 31(1):13-20.

103. Wang W, Caldwell MC, Lin S, Furneaux H, Gorospe M (2000) HuR regulates cyclin A and cyclin B1 mRNA stability during cell proliferation. *EMBO J* 19(10):2340-2350.

104. Singh G, Rebbapragada I, Lykke-Andersen J (2008) A competition between stimulators and antagonists of Upf complex recruitment governs human nonsense-mediated mRNA decay. *Plos Biology* 6(4):860-871.

105. Villanueva J, Yung Y, Walker JL, Assoian RK (2007) ERK activity and G1 phase progression: Identifying dispensable versus essential activities and primary versus secondary targets. *Molecular Biology of the Cell* 18(4):1457-1463.

106. Lai WS, Kennington EA, Blackshear PJ (2002) Interactions of CCCH zinc finger proteins with mRNA - Non-binding tristetraprolin mutants exert an inhibitory effect on degradation of Au-rich element-containing mRNAs. *Journal of Biological Chemistry* 277(11):9606-9613.

107. Okumura F, Zou W, Zhang DE (2007) ISG15 modification of the eIF4E cognate 4EHP enhances cap structure-binding activity of 4EHP. *Genes Dev* 21(3):255-260.

108. Shyu AB, Belasco JG, Greenberg ME (1991) Two distinct destabilizing elements in the c-fos message trigger deadenylation as a first step in rapid mRNA decay. *Genes Dev* 5(2):221-231.

109. Wu X, Chesoni S, Rondeau G, Tempesta C, Patel R, Charles S, Daginawala N, Zucconi BE, Kishor A, Xu G, Shi Y, Li ML, Irizarry-Barreto P, Welsh J, Wilson GM, Brewer G (2013) Combinatorial mRNA binding by AUF1 and Argonaute 2 controls decay of selected target mRNAs. *Nucleic Acids Res* 41(4):2644-2658.

110. Jing Q, Huang S, Guth S, Zarubin T, Motoyama A, Chen J, Di Padova F, Lin SC, Gram H, Han J (2005) Involvement of microRNA in AU-rich element-mediated mRNA instability. *Cell* 120(5):623-634.